ELUCIDATING THE INTERACTIONS OF THE GOLGI ASSOCIATED RETROGRADE PROTEIN (GARP) COMPLEX IN *ARABIDOPSIS THALIANA.*

RYAN MOEDT
BSc. University of Lethbridge, 2013

A Thesis Submitted to the School of Graduate Studies of the University of Lethbridge in Partial Fulfillment of the Requirements for the Degree

MASTER OF SCIENCE

Biological Sciences
University of Lethbridge
LETHBRIDGE, ALBERTA, CANADA.

PREPARATION OF THESIS

RYAN MOEDT

Date of Defence: August 25, 2015

Dr. E. Schultz Supervisor	Associate Professor	Ph.D.
Dr. J. Thomas Thesis Examination Committee Member	Professor	Ph.D.
Dr. I. Kovalchuk Thesis Examination Committee Member	Professor	Ph.D.
Dr. A. Russell Chair, Thesis Examination	Assistant Professor	Ph.D

This thesis is dedicated to my wife Amy, I could not have finished this without your constant love and support.

Abstract

Plants contain a diversified endomembrane system and transport within the network requires efficient and accurate vesicle transport. Tethering factors represent a group of loosely related proteins and protein complexes that act to physically link vesicles to the target membrane. UNH was previously identified as the VPS51 homolog of the Golgi-associated retrograde protein (GARP) complex, known to tether vesicles in endosome to trans-golgi network (TGN) retrograde transport. The *unh* cellular phenotype is similar to secretion/vacuole defects observed in yeast and metazoan GARP complex mutants suggesting a conserved function in plants. This study was designed to assess whether the *Arabidopsis* GARP complex members participate in similar protein interactions as found in other eukaryotes. All of the plant GARP subunits contain predicted N-terminal coiled coils, important for interaction in other organisms. We show through deletional mutagenesis that these predicted N-terminal coiled coils are required for UNH to interact with VPS52 *in vivo* via yeast two-hybrid.

Acknowledgements

I would like to thank Elizabeth Schultz for being an incredibly helpful supervisor and mentor despite numerous setbacks in the production of this thesis.

I would like to thank my family, especially my wife Amy for being supportive. You all provided the perfect combination of nature and nurture.

I would thank the members of the Schultz – Neema, Sabitree, Ai Me, Houlin, Kurt, Chahat, Bianca – you all made my time in the Schultz lab… interesting.

To all my friends that helped in different ways – Jordan, David, all the graduate students that offered advice, you're all more than appreciated.

A big thanks to my committee members – you offered great suggestions that helped in the production of this thesis.

Financial Support – Thanks to the University of Lethbridge for giving me the opportunity to complete my masters project.

Table of Contents

List of Tables

List of Figures

Abbreviations:

GARP: Golgi Associated Retrograde Protein

ER: Endoplasmic Reticulum

PM: Plasma Membrane

TIP: Tonoplast Intrinsic Protein

TGN: Trans-Golgi Network

EE: Early Endosome

PVC/MVB: pre-vacuolar complex/multivesicular body

RE: Recycling Endosome

NSF: N-ethylmaleimide sensitive factor

SNAP: Soluble NSF association protein

SNARE: SNAp (Soluble NSF Attachment protein) Receptor

TMD: Trans-Membrane Domain

SYP: SYntaxin of Plants

SM: Sec1/Munc18

VPS: Vacuolar Protein Sorting

GEF: Guanine nucleotide Exchange Factor

MTC: Multi-subunit Tethering Complex

COG: Conserved Oligomeric Golgi

CPY: CarboxyPeptidase Y

MPR: Mannose 6-Phosphate Receptor

IAA: Indole-3-Acetic Acid

UNH: UNHINGED

PCR: Polymerase Chain Reaction

All abbreviated protein constructs listed in table 3 (ex: UNH-DB).

Growth medium annotation:
Any growth medium lacking an amino acid features a minus sign prior to amino acid abbreviation. E.g. –his = media lacking histidine.

List of protein homologs

(plant/yeast/human)

UNH/VPS51/Ang2

SYP41/tlg2p/SYX16

SYP61/tlg1p/SYX6

AtRab6A/ypt6/Rab6B

1.0 Introduction

1.1 Cell polarity controlled by vesicle transport within the endomembrane system.

In unicellular and multicellular organisms, the asymmetric distribution of cellular constituents establishes cell polarity, a process vital for tissue patterning, cell division, development and cellular communication (Dettmer and Friml 2011). Most cells exhibit asymmetry to some extent, but certain specialized cell types have more obvious and functionally important polarity and they have received extra attention. For example, the organization of axons and dendrites within neurons highlights the importance of polarized growth between networks of cells (Tahirovic and Bradke 2009). Epithelial cells are another example of the asymmetric distribution within the cell as they must maintain apical-basal polarity in order to properly separate biological compartments (Yeaman et al. 1999). Plants also utilize cell polarity to control a number of processes such as organogenesis, tropic response and tissue development (Dettmer and Friml 2011). Auxin or indole-3-acetic acid (IAA) is an important plant hormone for plant development as its polar distribution helps to control cell division, differentiation and elongation (Zhao 2010). For example, the polar distribution of the auxin efflux PIN proteins drives the polarized transport of auxin within files of cells to establish a high auxin concentration necessary to induce cell differentiation into veins (Sachs 1981). The elongation of the pollen tube down to the ovule is another example of the importance of cell polarity. Pollen tubes exhibit highly polarized tip growth which requires the constant establishment of a defined growth site via specific vesicle transport (Li et al. 1999). Cell

polarity is necessary in all eukaryotes and is accomplished largely through complex vesicle transport networks within the endomembrane systems (Orlando and Guo 2009).

One of the characteristics of eukaryotes is their diversified endomembrane system. Distinct membrane enclosed organelles allow for the compartmentalization of various reaction conditions, driving a wide range of cellular processes. Eukaryotes share a basic framework for their endomembrane, including the endoplasmic reticulum (ER), Golgi apparatus, endosomes, vacuole and plasma membrane (PM), with each membrane being characterized by a unique set of proteins and lipids (Moreau et al. 2007). In order to transmit extracellular signals, transport proteins and control compartment identity, a highly dynamic transport system within the cell is required. To achieve this, cargo and signals are transported via small, membrane enclosed vesicles that bud from a donor compartment and fuse to the acceptor membrane (Hawes et al. 1999). Anterograde vesicle transport occurs when newly synthesized proteins that are translocated into the ER lumen follow a path to the Golgi apparatus where they are then sorted to the plasma membrane or vacuole (Denecke et al. 1990). Retrograde vesicle transport is a term used to describe the recycling of cargo back to its original location (Moreau et al. 2007). Retrograde transport of membrane components and signalling proteins is essential in maintaining the correct membrane composition of the donor compartment (Moreau et al. 2007). Though eukaryotes share many of the same basic endomembrane processes, there exists an enormous diversity in membrane composition, trafficking pathways and organelle function.

1.2 The role of the ER, Golgi apparatus and vacuole in cargo trafficking

The ER is organized as a single enclosed network of tubules and flattened sacs. Translocated proteins that are destined for secretion contain an ER signal sequence that brings the ribosome to the ER membrane (Alberts et al. 2002). The ER lumen contains

resident proteins that help fold and glycosylate trans-located proteins before they are transported on to the Golgi apparatus (Cooper 2000). In cereals and grasses, the ER lumen does not just function in processing but can store concentrated amounts of protein that segregate into unique storage compartments (Hawes and Satiat-Jeunemaitre 2005).

Typically, the Golgi apparatus consists of enclosed flattened sacs that are present as polarized stacks within the cell. Proteins enter the convex *cis* face and are shuttled towards the concave *trans* face where they exit. The carbohydrate additions of proteins are modified along the way (Cooper 2000). In this way, the Golgi apparatus acts as a factory, correctly modifying proteins and shipping them to their correct destination. Transport between the ER-Golgi interface also appears to be different in plants compared to animals. In animal cells, the Golgi apparatus is a stationary compartment with a particular location in the cell. Transport between the ER and Golgi occurs mainly via vesicle transport along microtubules (Presley et al. 1997). Plants have evolved a unique Golgi network consisting of much smaller, motile Golgi stacks that are distributed throughout the cytosol (Marty 1999; Boevink et al. 1998). In plants, ER-Golgi transport can occur via vesicles, but may also occur via a type of transport not yet observed in other organisms. The numerous Golgi stacks can move along the ER via actin cables, picking up cargo along the way (Boevink et al. 1998; Brandizzi and Wasteneys 2013). It is currently unclear how important this adaptation is to plant function.

Proteins incorrectly folded, along with an array of intracellular cargo, are transported to the lytic vacuole/lysosome for degradation. The Golgi transports hydrolytic enzymes to the vacuole that aid in the breakdown of a wide variety of substances (Cooper 2000). In addition to protein degradation, plants contain a diversified vacuole system to aid in nutrient storage and the regulation of turgor pressure. In plants, storage of various proteins and nutrients allows for the growth of germinating seeds and rapid expansion of tissue following periods of dormancy. Plants have thus evolved effective mechanisms of

storage in their embryonic and vegetative cells (Herman and Larkins 1999). Plants distinguish between these different vacuole types by the composition of their membranes. For example, α-TIP (tonoplast intrinsic protein) defines the storage vacuole whereas y-TIP defines a distinct lytic vacuole (Vitale and Raikhel 1999). Both types of vacuoles can be present in the same cell, each with independent transport routes (Marty 1999; Pedrazzini et al. 2013).

1.3 Trans-Golgi Network and Early Endosome

The trans-Golgi network (TGN) and endosomes function as major sorting hubs for endocytosed cargo and proteins originating from the *cis*-Golgi. The TGN contains sorting signals, vesicle coat components and other important lipids and proteins for modifying and shuttling various cargo to their subcellular locations (Gu et al. 2001). Endosomes work in close concert with the TGN and act in a conserved manner within all eukaryotes by sorting endocytosed products from the plasma membrane and external environment as well as carrying cargo to the lytic vacuole for degradation (Contento and Bassham 2012). Endosomes are further subdivided into three unique categories: the early endosome (EE), the recycling endosome (RE) and the late endosome or pre-vacuolar complex/multivesicular body (PVC/MVB). The early endosome is the first location for endocytosed products. Endocytosed products can then be recycled to the plasma membrane via REs or be sent for degradation in the lytic vacuole via the PVC/MVB (Contento and Bassham 2012).

Despite this simplified categorization of compartments, the actual classification and function is difficult to compare between eukaryotes. In animal cells, the early endosome is the initial location for endocytosed proteins and acts as an endosomal

sorting hub. In animals, the TGN is simply a sub-region of the Golgi apparatus whereas in plants, the TGN is present as an independent organelle and functions as the main sorting hub for endocytosed and secretory proteins (Viotti et al. 2010; Uemura et al. 2004). Thus, the role of the early endosome is fulfilled by the TGN, now aptly named the TGN/EE (Contento and Bassham 2012; Dettmer et al. 2006). Though plants do not contain a distinct early endosome, the PVC/MVB is present. However, it appears that the composition of the plant PVC/MVB may also be unique. For example, Rab5 is an EE marker in mammalian cells but the plant homologs, AtRABF2b and AtRabF2a, have been localized to the PVC/MB in *Arabidopsis* (Lam et al. 2007).

The endomembrane system of all eukaryotes is a highly dynamic and precise intracellular transport network, with unique features appearing in many different organisms. Analysis of how cells regulate trafficking has uncovered an array of different proteins that take part in a multi-step process from cargo selection and vesicle budding to dissociation and recycling of key proteins after membrane fusion. The precision of vesicle transport is controlled by a large repertoire of proteins including coat proteins, SNAREs, Rab GTPases and tethering factors (Cai et al. 2007). One would expect that due to the differences in endomembrane networks between eukaryotes, the machinery that controls the transport pathways would have evolved novel interactions. Indeed, we observe that plants have undergone large expansions of the protein families related to vesicle transport. This suggests that unique functions and interactions may have evolved in plants. Here I will discuss current knowledge on vesicle transport machinery and hypothesize various transport mechanisms in plants.

1.4 SNARE protein function and classification

Once a vesicle has budded from the donor membrane it has two important tasks: specific membrane targeting and subsequent fusion. Both processes are driven in part by the SNARE protein family. SNARE proteins contain two important features, a C-terminal transmembrane domain (TMD) for anchoring and an N-terminal SNARE domain which consists of a heptad repeat of 60-70 amino acids forming a coiled-coil domain. Key residues for function within the SNARE domain, arginine and glutamate, led to the classification of R-SNAREs and Q-SNAREs, respectively (Sutton et al. 1998). R-SNAREs form a relatively small group and are commonly found on incoming vesicles, while the Q-SNAREs are more diverse and are typically present on donor membranes. Q-SNAREs are further subdivided into three distinct groups: Q_a, Q_b, and Q_c SNAREs. In most cases, a single R-SNARE interacts with each type of Q-SNARE, forming the Q_{abc}R-complex that helps to drive membrane fusion (Bock et al. 2001).

Interactions are generally quite specific between different SNARE sets and this specificity helps to target vesicles with particular R-SNAREs to particular organelles with the correct Q_{abc}-SNARE complex (Bock et al. 2001). Eukaryotes have undergone a large diversification of SNARE proteins leading to a high number of possible SNARE interactions, especially in plants. For example, *Arabidopsis thaliana* contains 60 SNAREs compared to 25 in yeast and 36 humans (Lipka et al. 2007). The increase is due to an expansion in the existing SNARE families, with the SYntaxin in Plant (SYP) 7 family being the only new isoform (Lipka et al. 2007). Despite the expanded families, it appears many of the family members are not redundant. Individual mutations to SYP111, SYP21, SYP22, SYP41 and SYP42 are all homozygous lethal (Sanderfoot et al. 2000). Additionally, individual SNAREs within a given family appear to be differentially

expressed and many have unique localizations within the cell (Lipka et al. 2007). It appears that in many cases expansion to existing SNARE families has allowed different members to evolve novel functions within different tissues.

1.5 The mechanism of SNARE mediated vesicle fusion

Understanding vesicle fusion in eukaryotes first began with the discovery of two important proteins; N-ethylmaleimide sensitive factor (NSF) and α -SNAP (soluble NSF association protein) (Clary et al. 1990; Glick and Rothman 1987). Their role in membrane fusion was first hypothesized after showing that inactivation of NSF caused vesicles to start accumulating on the Golgi membranes (Malhotra et al. 1988). It was hypothesized that these proteins acted in concert with other unidentified protein members to facilitate membrane fusion. Sollner *et al* identified three important proteins associated with the NSF/α -SNAP complex, thus discovering the SNARE protein family (Söllner et al. 1993). Crystallography studies revealed that ionic interactions between the carboxyl of glutamate and guanidino group of arginine form a type of lock surrounded by an inner hydrophobic coiled-coil seal. Two adjacent SNARE complexes 'zip' together from the N-terminal region towards the C-terminal, twisting the helices and forcing the membranes to fuse together (Sutton et al. 1998). Most commonly, 3 SNARE proteins on a target membrane each contribute a helix to form a groove in which a single SNARE helix on an incoming vesicle can bind to form a trans-SNARE complex. This trans-SNARE complex helps to drive the energetically unfavorable process of membrane fusion (Rothman 1994).

1.6 Regulation of SNARE proteins

Q_a-SNAREs are also termed syntaxins, due to high sequence similarity in their SNARE domain, but many also contain an additional tri-helical N-terminal domain (H_{abc}) (Fernandez et al. 1998; Sanderfoot et al. 2000). The H_{abc} domain can bind to its own SNARE domain, inhibiting association with other SNAREs. The H_{abc} domain, along with an N-terminal peptide sequence, act as regulatory domains, typically interacting with Sec1/Munc18 (SM) proteins to either facilitate or inhibit SNARE fusion (Furgason et al. 2009; Fiebig et al. 1999). In yeast for example, the Sec1/Munc18 (SM) protein Sly1 binds to the regulatory domain of the syntaxin Sed5 and relaxes the auto-inhibitory closed conformation (Demircioglu et al. 2014). Many other modes of interaction are also observed and appear to be quite diverse. For example, the SM protein VPS45p binds to the syntaxin tlg2p via two modes of interaction: it can bind to the N-peptide as well as the closed conformation of tlg2p, though the function of these different interactions is unclear (Furgason et al. 2009).

1.7 Rab GTPases: their role as molecular switches

Despite the complex regulation observed in SNARE proteins, a plethora of experiments revealed that the action of SNAREs was insufficient to account for the highly specific vesicle transport seen in higher eukaryotes. Vesicle fusion was seen to occur in distinct regions within the endomembrane system despite the fact that SNAREs were evenly distributed. Brennwald *et al* (1994) revealed in yeast that two SNAREs, Sso1p and Sso2p, were relatively homogenous across the plasma membrane, yet exocytic vesicles only fused at the budding tip (Brennwald et al. 1994). Additionally, vesicle fusion occurred at a much slower rate *in vivo* compared to *in vivo*, suggesting additional factors are required to accelerate the process (Fasshauer et al. 2002). It was revealed that

small Rab GTPase proteins act in concert with many proteins, such as SNAREs, to facilitate vesicle budding, tethering, and fusion.

Rab GTPases form the largest sub-family of the small Ras-like GTPases. They mainly function as signalling proteins by cycling through active/inactive states via binding of GTP and hydrolysis to GDP, respectively (Takai et al. 2001). Once a Rab protein is translated, the GDP-bound form undergoes prenylation of C-terminal cysteine residues with two geranylgeranyl groups. The modified cysteines are then embedded in their correct membrane with the help of other regulatory proteins (Hutagalung and Novick 2011). A guanine nucleotide exchange factor (GEF) can then convert the Rab to its GTP-bound, or active state. It is the active, membrane bound Rab GTPase that can then interact with various effectors (proteins that preferentially bind to a GTP-bound Rab) to help facilitate various steps in vesicle trafficking (Hutagalung and Novick 2011). Rab GTPases are termed the master regulators of vesicle transport as they have a role in almost every vesicle trafficking step.

Rab GTPases have experienced a large expansion and diversification in multicellular organisms: there are 11 identified Rab GTPases in yeast while Arabidopsis and humans contain 57 and 60 different Rabs, respectively (Woollard and Moore 2008; Pereira-Leal and Seabra 2001). The Arabidopsis Rabs fit into 18 functional subclasses whereas humans have about 41 functional subclasses (Rutherford and Moore 2002; Pereira-Leal and Seabra 2000). Plants and humans share only 8 functional subclasses, suggesting a diversification of Rabs in both plants and animals (Rutherford and Moore 2002). For example, the Rab7 class in mammals contains a single member involved in vacuolar vesicle transport whereas the Arabidopsis AtRABG subfamily is related to Rab7

but contains 8 members possibly reflecting the increased complexity of the plant vacuole system (Vernoud et al. 2003).

1.8 Classification of vesicle tethering factors

Pfeffer first identified three tethering factors activated by Rab GTPases that mediate the initial attachment of vesicles to their target membranes: rabaptin-5, p115/Uso1 and the exocyst complex (Pfeffer 1996). This finding led to the classification of two groups of tethering factors, not related through structure but through function: 1) a long, coiled-coil protein family and 2) a class of large multi-subunit tethering complexes (MTCs) (Whyte and Munro 2001). Seven conserved complexes exist within the MTC class; the quatrefoil group contains 4 MTCs (exocyst, COG, GTC and GARP) with most subunits sharing a similar N-terminal domain, while the other 3 MTCs (TRAPP, Class C VPS and Ds11p) have no structural similarity but functional (Whyte and Munro 2002). I will describe only the quatrefoil group further.

1.9 Quatrefoil tethering complexes – The Exocyst/COG complex

Exocytosis is an important trafficking event that mediates the secretion of intracellular cargo important for cell polarization, growth, and communication. The exocyst complex is composed of eight subunits and acts to tether vesicles from the post-Golgi (TGN) destined for secretion to active sites of secretion on the plasma membrane (He et al. 2007). The exocyst interacts with a plethora of proteins associated with vesicle transport such as different Ras-like GTP-binding proteins including Rab, Rho, Arf and Rals (Novick and Guo 2002).

Compared to yeast and mammals, relatively little is known about exocyst function in plants. Plants appear to contain homologs to all of the exocyst subunits, but they exist as multiple copies, whereas most eukaryotic homologs exist as single genes (Hála et al. 2008). For example, *Arabidopsis* contains 23 EXO70 genes whereas humans and yeast only contain a single copy (Zhang et al. 2010). The yeast EXO70 subunit links vesicles to the PM by binding to phosphatidylinositol 4,5- bisphosphate whereas *Arabidopsis* EXO70B2 interacts with SNAP33 SNARE via a yeast two-hybrid assay (He et al. 2007; Pečenková et al. 2011). The SEC3 subunit of the exocyst in Arabidopsis was also shown to interact with Rho GTPases via binding to the adaptor protein ICR1 (Hála et al. 2008). Mutations to certain exocyst subunits reveal defects in pollen tube growth as well as defects to etiolated hypocotyl elongation, consistent with defects to vesicle targeting in other eukaryotes (Hála et al. 2008). Despite some functional conservation of the plant exocyst in vesicle trafficking, the exocyst size, associations and family member expansion differs compared to yeast and mammals, suggesting unique functions may have evolved in plants (Hála et al. 2008).

The conserved oligomeric Golgi (COG) complex is another tethering complex member that functions to tether vesicles in retrograde transit within the Golgi apparatus (Wuestehube et al. 1996). The COG complex has been shown to interact with a plethora of various Rab GTPases, SM proteins, SNAREs, motor and coat proteins in both yeast and mammals (Suvorova and Lupashin 2002). In Arabidopsis our knowledge of the COG complex is very limited. So far, the COG complex has only been shown to interact with the EXO70 subunit of the exocyst via a yeast two-hybrid assay (Willett et al. 2013). It is

currently unclear whether the plant COG complex functions in a similar way compared to yeast and mammalian models.

1.10 Role of the GARP complex in eukaryotes

A series of carboxypeptidase Y (CPY) and late Golgi protein missorting defects in *S. cerevisiae* led to the discovery of the Golgi associated retrograde protein (GARP) complex which is involved in endosome to late Golgi transport and was originally thought to consist of three subunits (VPS52/53/54) (Conibear and Stevens 2000). The three subunits associate into a 1:1:1 complex that is destabilized in the absence of any single member, leading to phenotypically indistinguishable mutants in yeast (Conibear and Stevens 2000). A fourth subunit, termed VPS51, was discovered later with a similar, albeit weaker mutant phenotype than the other subunits (Conibear et al. 2003; Siniossoglou and Pelham 2002). VPS51 is not a required subunit for complex formation, but does seem to have a role in further stabilizing the complex (Siniossoglou and Pelham 2002). GARP mutants show improper recycling to the TGN of two important proteins, the v-SNARE Snc1p and the CPY cargo receptor Vps10p, originating from the early and late endosome, respectively (Conibear et al. 2003). The inability to recycle VPS10p stops the hydrolase CPY from reaching the vacuole and it is instead secreted. Substances that would normally be degraded build up in the vacuole, leading to size and function defects in the vacuole (Conibear and Stevens 2000).

The GARP complex is conserved across all eukaryotes, with similar vacuolar/lysosomal transport defects occurring in plant, mammalian and nematode models (Luo et al. 2011; Pérez-Victoria et al. 2008; Conibear and Stevens 2000). In mammals mutant for any core GARP subunits, the acid hydrolase precursor, cathepsin D,

is improperly secreted. The GARP complex is responsible for the retrograde transport of mannose 6-phosphate receptors (MPRs) which normally carry a cathepsin D precursor from the TGN to the endosome (Pérez-Victoria et al. 2008). MPRs accumulate in small vesicles that are in transit downstream of the endosome. The inability to recycle MPRs arrests further transport of cathepsin D to the vacuole in a manner similar to the improper CPY secretion seen in yeast (Pérez-Victoria et al. 2008). In plants, mutation to the GARP complex can cause the AFVY peptide, which is normally targeted to the vacuole, to be improperly secreted (Pahari et al. 2014). The *Arabidopsis* VPS52/POK subunit has been shown to associate in a large complex that is bound to cell membranes and localizes to vesicles associated with the Golgi apparatus and PVC (Guermonprez et al. 2008). Additionally, the *Arabidopsis* VPS53/HIT1 is able to partially rescue the yeast heat intolerant *vps53*Δ null mutant, suggesting a conserved biological function between the two subunits (Wang et al. 2011). These results suggest that the *Arabidopsis* GARP complex functions in a similar manner to mammalian and yeast counterparts.

The GARP complex causes general cellular defects to vacuolar targeting, but mutations to the subunits display a range of different phenotypes at the organismal level. In wobbler mice, a single VPS54 hypomorphic (L967Q) mutant can cause severe motor neuron degeneration, due to lower levels of GARP, while a complete knockout leads to embryonic lethality (Schmitt-John et al. 2005; Pérez-Victoria et al. 2008). In *Arabidopsis*, a single Ser-to-Tyr substitution within VPS53 causes the *hit1-1* phenotype which leads to reduced tolerance to heat and water stress (Lee et al. 2006). VPS52/53/54 T-DNA insertion mutants, presumed to result in a null phenotype, result in male gametophyte transmission defects thought to be caused by improper pollen tube formation, though

transmission ratios suggest some of the mutants are embryonic lethal at a very early stage (Guermonprez et al. 2008). The increasingly severe phenotypes that occur in more complex eukaryotes may be due to a greater necessity for precise intracellular transport within specialized cells. For example, cells that require finely tuned vesicle transport such as motor neurons and pollen tubes are most severely affected by GARP mutations, as seen by neural degeneration and pollen tube growth defects in mice and plants, respectively (Lobstein et al. 2004; Guermonprez et al. 2008; Pérez-Victoria et al. 2008). It seems that despite a conserved function in endosome to TGN retrograde transport, the consequence of defective retrograde transport differs between different cell types of different organisms.

1.11 The interactions of GARP with vesicle trafficking related proteins

Our understanding of how the GARP complex controls endosome to TGN trafficking is still relatively unclear. In order to understand the role of the GARP complex in plants, it is important to identify which proteins the GARP subunits interact with and which domains within the subunits are important to carry out its function. So far, studies have only been done in yeast and mammalian models. There are two important regions in each GARP subunit defined by an N-terminal region consisting of coiled-coil domains, and a much less conserved C-terminal region with varying function (Liewen et al. 2005; Siniossoglou and Pelham 2002). In both yeast and mammals, the GARP subunits are stabilized through the presence of N-terminal coiled-coil domains, creating a 4 coiled bundle reminiscent of the 4 helical trans-SNARE complex (Liewen et al. 2005; Siniossoglou and Pelham 2002). Interestingly, expression of the yeast N-terminal coiled coil domains of VPS52, VPS53 or VPS54 alone was not enough for the GARP complex

to assemble *in vivo* via a GST (glutathione S-transferase) pull-down assay, though the SNARE helices alone could form a complex (Siniossoglou and Pelham 2002). The exact role of the C-terminal domains is still unclear, but they may be involved in assembling the complex, in localization or in interaction with other factors such as SNAREs and GTPases.

In the *vps54* yeast mutant, the N-terminal domain of VPS54 can restore CPY targeting (late endosome cargo), but is not able to retrieve Snc1 (early endosome cargo) (Quenneville et al. 2006). The C-terminal VPS54 also associates with the early endosome, suggesting a possible role in localization of the GARP complex to the early endosome (Quenneville et al. 2006). It has also been shown in humans that the N-terminal coiled-coil domains of both VPS53 and VPS54 can bind to the Stx6/Stx16/Vti1a TGN SNARE complex via GST pull-down assay but require the C-terminal domain for the initial tethering process (Pérez-Victoria and Bonifacino 2009).

In yeast, the assembly and regulation of the GARP complex is quite well characterized. The Rab GTPase YPT6 is activated by the heterodimeric Ric1p-Rgp1p GEF, a peripheral membrane protein restricted to the late Golgi (Siniossoglou et al. 2000). Once activated, YPT6-GTP interacts with VPS52 to recruit the GARP tethering factor complex (Figure 1). Interestingly, AtRab6A has been shown to complement and rescue the *ypt6* mutant in yeast, suggesting a possible conserved role in plants and yeast (Bednarek et al. 1994). The GARP complex then associates with t1g1p SNARE protein, which is localized to the late Golgi and endosomes, though its exact role in fusion is not known (Figure 1)(Siniossoglou and Pelham 2001). VPS51 binds to the H_{abc} domain of tlg1p via an N-terminal helix. Additionally, crystallography revealed that VPS51 requires

a somewhat conserved phenylalanine/tyrosine (di-tyrosine in mammals) motif for this interaction (Fridmann-Sirkis et al. 2006; Abascal-Palacios et al. 2013). These studies provide an attractive model for endosome to late Golgi transport. The GARP complex tethers vesicles at the endosome and VPS52 recruits them to the late Golgi via interaction with ypt6-GTP. VPS51 then binds to the H_{abc} domain and activates tlg1p, allowing the SNARE complex to facilitate membrane fusion. These interactions appear to be conserved in humans as VPS51 interacts with SYX6 (tlg1p homolog) and VPS52 interacts with the ypt6 homolog, Rab6 (Figure1)Abascal-Palacios et al. 2013; Monier et al. 2002).

1.12 Role of UNHINGED within the GARP complex

Pahari *et al* (2014) identified *UNH* as the VPS51 homolog in *Arabidopsis*. UNH has a conserved VPS51 domain (pfam08700), determined by sequence similarity, of about 85 residues that shows similarity to exocyst and COG subunits. UNH also shares a highly conserved central sequence 'LVYENYNKFISATDT' motif within the VPS51 domain that is found in most VPS51 homologs, except yeast. Yeast VPS51 encodes a small protein (~150aa), whereas metazoan homologs and UNH, are much larger (>700aa). Pahari *et al* (2014) showed through yeast two-hybrid analysis that VPS51 interacts with the VPS52 subunit of the GARP complex, similar to interactions observed in yeast and humans (Pérez-Victoria et al. 2010; Siniossoglou and Pelham 2002). All VPS51 homologs share similarity in their N-terminal domains with considerably less similarity in the C-terminal region. Though the plant GARP complex appears to function in a similar manner to that in yeast, it is unclear whether UNH interacts with similar SNAREs as do yeast and animal VPS51. Pahari *et al* (2014) revealed that UNH was not

able to interact with SYP41, SYP22, Vti11 or AtRab6A via yeast two-hybrid. VPS51 in yeast and humans interacts with tlg1p and SYX6 respectively so it would be interesting to test whether UNH interacts with the *Arabidopsis* homolog SYP61, or SNAREs such as Vti12 and SYP51 that form SNARE complexes with SYP61 or with the ypt6 homolog, AtRab6A (Sanderfoot et al. 2000).

1.13 Detecting Protein Interactions

In order to detect interactions between the GARP complex and other vesicle trafficking related proteins a number of different methods can be used. Both yeast two-hybrid and bimolecular complementation assays can be used to detect protein interactions *in vivo* and *in planta*. These assays utilize a split protein system in which interaction between two proteins of interest is necessary for reconstitution of the split protein. In the yeast two-hybrid, proteins are fused to either the activating domain (TA) or DNA binding domain (DB) of the GAL4 protein (Fields and Song 1989). If interaction is seen in the yeast nucleus, the GAL4 protein will come together and turn on expression of a reporter gene (Fields and Song 1989). The bimolecular fluorescence complementation assay works by translationally fusing two proteins to either the C-terminal half of the EYFP (yellow fluorescent protein) or the N-terminal EYFP (Lee et al. 2008). These proteins are then infiltrated into tobacco via *Agrobacterium tumefaciens* and interaction of the proteins allows for reconstitution of the EYFP. The fluorescence is then detected in tobacco epidermal cells via confocal microscopy.

1.14 Objectives

UNHINGED (UNH) is a VPS51 homologue and its exact role in retrograde transport in plants is unclear. The overall objective of this thesis is to uncover how VPS51 functions to control retrograde transport from the endosome to the TGN in *Arabidopsis.* Pahari *et al* previously showed that UNHINGED interacts with VPS52 based on yeast two-hybrid analysis. Similar mutant phenotypes suggest that the plant GARP complex appears to function in a similar way to its mammalian and yeast counterparts, thus it may interact with the plant homologs of both tlg1p and ypt6. I hypothesize that UNH contains similar motifs and domains important for interaction in yeast and mammals, and interacts with the plant homologs in a similar manner. I also hypothesize that conserved N-terminal coiled coil domains will exist in the Arabidopsis GARP subunits and be important for complex assembly and stability.

2. Materials and Methods

2.1 *In silico* analysis of GARP complex subunits

UNHINGED was analyzed *in silico* to predict possible protein interactions using a number of different programs. Sequences of *M. musculus* VPS51 (UniProtKB: Q3UVL4), *H. sapiens* Ang2/VPS51 (UniProtKB: Q9UID3), *D. rerio* VPS51/ffr (UniProtKB: Q155U0), *S. cerevisiae* VPS51/YKR020W (UniProtKB: P36116), *C. elegans* VPS51/B0414.8b (UniProtKB: G8XYY4) were aligned using ClustalW multiple sequence alignment (Gap Open: 10, Gap Extension: 0.2, Gap distance; 5, No gap ends, NJ clustering) and Boxshade (RTF new, 0.5 fraction for shading) was used to generate a comparison map (Figure 2). ClustalW allows for the alignment of multiple DNA or protein sequences while BOXSHADE allows for the shaded visualization of the ClustalW results. BOXSHADE analyzes all the sequences submitted and generates a consensus sequence based on the number of identical amino acids present in the inputted sequences. The fraction of identical amino acids needed to generate a consensus amino acid is defined by the user. Once the consensus sequence is determined all other amino acids are shaded based on similarity to it with exact matches being shaded black and similar amino acids being shaded grey. Possible coiled-coil regions were predicted using COILS server: http://www.ch.embnet.org/software/°COILS_form.html. COILS is a program that predicts the probability of a coiled coil region by comparing different heptad repeat sequences within a given protein to known coiled coil heptad repeats. Stable coiled coil structures are generally found to contain at least four heptad repeats, so a window size of 28 amino acids is generally used. Window sizes of 14 and 21 amino acids are also calculated as a coiled coil could be stabilized by nearby helices or

structures (Lupas et al. 1991). Each amino acid in a given window is given a score based on its similarity to amino acids in previously characterized coils. When a coil is predicted, a higher number of amino acids that match known coil structures will result in a higher probability score for that coil.

2.2 *Escherichia coli* competent cells

A starter culture was made by inoculating 50 mL of YENB with a single DH5α *E. coli* colony and growing the culture at 37°C overnight in a shaking incubator at 275 rpm. 2.5 mL of starter culture was used to inoculate 6x 500 mL flasks with 250 mL YENB. The cultures were grown until an OD_{600} of 1.0 was reached. Cells were then placed on ice and spun down in pre-chilled bottles in a pre-chilled centrifuge at 2000 g for 10 minutes. Each pellet was washed with 25 mL of cold, sterile water and then pooled together and spun down at 2000 g for 10 minutes. Pellets were then repeatedly (x2) washed until the supernatant had no remaining salts (clear) with 200 mL of cold, sterile water and re-spun for 10 minutes at 2000 g. The remaining pellet was re-suspended in 30 mL 10% glycerol and spun down as described above before being gently re-suspended in 4 mL of 10% glycerol. Cells were then dispensed into 100 µL aliquots and dropped into liquid nitrogen before being stored at -80°C.

2.3 *Agrobacterium tumefaciens* competent cells

A single colony of the gv3101 strain of *A. tumefaciens* was inoculated into 2 mL of YEP media supplemented with 25 mg/mL of gentamycin and shaken at 250 rpm, at 28°C. The overnight culture was then added to 200 mL of YEP + gentamycin and shaken at 250 rpm at 28°C until an OD_{600} of 0.3 was reached (4-5 hours). Cells were then

spun down at 4°C at 5000 rpm for 10 minutes. The pellet was re-suspended three times in 20 mL cold, sterile filtered 1 mM HEPES pH 7 and spun down using the same conditions as above. The pellet was then re-suspended in 2 mL of ice cold 10% sterile glycerol. The resuspension was then dispensed into 100 µL aliquots and stored at -80°C.

2.4 All-in-one miniprep method

1.5-2 mL of bacterial culture was pelleted at 7000 rpm for 1 minute. The pellet was re-suspended in 150 µL extraction buffer (5% sucrose, 50 mM EDTA, 50 mM Tris pH 8, 0.75 NH_4CL, 0.5% Triton X-100, lysozyme 100 µg/mL, RNase 25 µg/mL). The suspension was incubated at 65°C for 5 minutes then centrifuged for 10 minutes at max RPM. 120 µL isopropanol was added and subsequently centrifuged at 7000 rpm for 10 minutes. The supernatant was discarded and the pellet was washed with ethanol 70% before being dissolved in TE buffer.

2.5 Electroporation of *A. tumefaciens* and *E. coli*.

All bacterial and *Agrobacterium* plasmid constructs were transformed via electroporation using the Eppendorf electroporator 2510. Competent cells were thawed on ice for five minutes before <1 µL of plasmid/ligation mix was added. The cells were then immediately added to chilled 2 mm gap cuvettes for both *E. coli* and *A. tumefaciens* and pulsed at 1800 V for *E. coli* and 2500 V for *A. tumefaciens*. For optimal efficiency, pre-warmed SOC media was immediately added to the cuvette and the cells were transferred to a 1.5 mL Eppendorf tube before incubation. *E. coli* was incubated at 37°C, 275 rpm for 1 hour while *Agrobacterium* was incubated at 28°C, 225 rpm for 2-4 hours.

50-200 µL of cells were then spread onto plates containing the appropriate antibiotic and incubated overnight at 37°C for *E. coli* or 2 days at 28°C for *Agrobacterium*.

2.6 *Saccharomyces cerevisiae* competent cells and transformation

YPB2 [MATa, *ura3-52, his3-200, ade2-101, lys2-801, trp1-901, leu2-3, 112 canR, gal4-542, gal80-538, LYS1::GAL1-HIS3, URA3:: (GAL4$_{17mers}$)-LacZ]*

The *S. cerevisiae* strain YPB2 was inoculated into 5 mL liquid medium (SD or YPAD media) and incubated overnight in 25 mL flasks (to avoid sedimentation) at 30°C and 200 rpm. To determine the titer of the initial yeast culture the number of cells were counted using a haemocytometer. 10 µL of the culture was pipetted between the haemocytometer groove and the cover slip until the cells covered the grid. Yeast cells were counted using a Nikon Eclipse E600 microscope. The correct inoculation volume of the overnight culture was then added to 50 mL pre-warmed SD media to give a final concentration of 5 x 10^6 cells/mL. After completing two division cycles and reaching a titer of at least 2 x 10^7 cells/mL (4-5 hours), cells were harvested at 3000g for 5 minutes. Cells were washed with 25 mL of water and then transferred to a microfuge tube and washed again with 1mL of water. The pellet was then re-suspended in 1 mL water and aliquoted to 100 µL amounts (approximately 10^8 cells). For each transformation, 100 µL of yeast culture was spun down to obtain a pellet. The transformation mix (240 µL PEG 50%, 36 µL LiAc 1.0 M, 50 µL salmon sperm DNA, 34 µL plasmid DNA + water to a total of 360 µL) was added to the pellet and vortexed before incubation at 42°C for 40 minutes. The transformation mix was centrifuged at max speed (13000 g) and the supernatant was aspirated before being re-suspended in water. The yeast transformation was then plated onto selective SD media and allowed to grow at 30°C for 3-5 days.

2.7 Primer design for cDNA PCR amplification.

Primers for all cDNA amplifications were designed using either Primer-BLAST or by manual design (Ye et al. 2012). The following *A. thaliana* cDNAs used in each PCR were obtained from ABRC and RIKEN: UNH (pda19438), VPS52 (pda01753), VPS53 (pda19355), VPS54 (pda08404), SYP41 (182L15), SYP51 (U21517), SYP61 (C104896), SYP71 (U82333), and Vti12 (U60796). For the yeast complementation test, UNHINGED cDNA was amplified using pYES primers designed to incorporate intrinsic EcoRI and KpnI sites and a yeast consensus sequence at the translation initiation site (table 1). Pahari *et al* (2014) had previously constructed UNH-DB, VPS52-TA, VPS53-TA, VPS54-TA, vti11-TA, SYP41-TA, SYP22-TA, and AtRab6A-TA. For additional constructs, cDNAs for the yeast two-hybrid assay were amplified using primers with intrinsic restriction cut sites. As well the forward primer was designed to maintain the reading frame through the C-terminal of the GAL4 gene to the start of the gene of interest (table 1). For the BiFC assay, UNHINGED, VSP52 and SYP61 cDNAs were amplified using specific pSAT primers (table 1) containing SalI and KpnI restriction sites. Reverse primers for each gene had altered stop codons to allow read-through into the fluorescent protein.

2.8 PCR conditions: standard and around-the-world

Phusion polymerase (New England Biolabs) was used for sequencing and cDNA amplifications for cloning with the following PCR conditions: 0.5 µM primer, 1.5 mM Mg^{2+}, 50 mM Na^{+}, 0.2 mM dNTPs, (34 cycles of 98°C 30 s, Primer T_m 30 s, 72°C 30 s/kilobase). For colony PCR, primers in the initial cDNA amplification step were used unless vector specific primers were available (table 2). ABM taq was used for colony

PCRs under the following conditions: 0.5 µM primer, 1.5 mM Mg^{2+}, 50 mM Na^{+}, 0.2 mM dNTPs; (34 cycles of 94°C 30 s, Primer T_m 30 s, 72°C 60 s/kilobase; colony PCRs have an initial 10 minute 94°C step).

Truncated cDNAs were generated using around-the-world PCR. Primers were designed to amplify outwards from UNH-pJet1.2 in order to delete certain regions of UNH (Figure 2): Primer_ATW_rightborder_Fwd + Primer_ATW_rightborder_rev5+6 for 1-118 aa and 1-289 aa respectively; Primer_ATW_leftborder_NewRev2 + Primer_ATW_leftborder_Fwd1+3 for 78-780 aa and 291-780 aa respectively.

2.9 Ligation into pJET1.2, Y2H, BiFC and complementation vectors.

Around-the-world PCR products were digested with DpnI for 3 hours at 37°C to remove original UNH-pJET1.2 uncut plasmids. The digested PCR product was then cleaned using the FroggaBio PCR clean up kit (Cat. # DF100) before overnight re-ligation of the truncated UNH mutant still in pJET1.2 (Thermoscientific).

All other PCR products were blunt end ligated into the pJET1.2 vector and positive transformants were selected using colony PCR with pJET1.2 specific primers (Table 2). Positive colonies were grown up at 37°C and 275 rpm in 5-10 mL LB supplemented with the vector specific antibiotic. The plasmid DNA was then extracted using the all-in-one mini-prep method (see above), digested with correct restriction enzymes and fragments were separated by gel electrophoresis to confirm the presence of the insert. cDNA inserts were gel extracted in TAE using the FroggaBio gel extraction kit (Cat. # DF100) before being ligated into the vectors listed below (3:1 insert:vector ratio) using T4 ligase (New England Biolabs) at 16°C overnight. The ligase was heat

inactivated at 80°C for 20 minutes before the ligation mixture was transformed into *E. coli* DH5α via electroporation (see above).

For the yeast complementation assay, UNH was ligated into the pYES2/CT vector to produce UNH-pYES2/CT. For the yeast two-hybrid assays, various cDNAs were ligated into pbi-770 (DB) or pbi-771 (TA) vectors to produce SYP51-TA, SYP61-TA, Vti12-TA, VPS52-DB, VPS53-DB, VPS52-DB, SYP61-DB, UNHΔ1-118aa-DB, UNHΔ1-289aa-DB, UNHΔ78-780aa-DB, and UNHΔ291-780aa-DB. For the BiFC assay, UNH was ligated into pSAT1A-nEYFP-N1 (CD3-1066) to produce pSAT1A-nEYFP:UNH. VPS52 and SYP61 were both ligated into pSAT4A-cEYFP-N1 (CD3-1079) to produce pSAT4A-cEYFP:VPS52 and pSAT4A-cEYFP:SYP61. Entire expression cassettes (double CaMV 35S promoter, cDNA-FP fusion) were excised using rare restriction enzymes (pSAT1A and with pSAT4A with AscI and I-SceI, respectively) and ligated into the binary vector pPZP-RCS2-ocs-bar-RI (pE3519, CD3-1058) to produce pPZP-RCS2-ocs-bar-RI:pSAT1A-nEYFP:UNH (UNH-nEYFP), pPZP-RCS2-ocs-bar-RI:pSAT4A-cEYFP:VPS52 (VPS52-cEYFP) and pPZP-RCS2-ocs-bar-RI:pSAT4A-cEYFP:SYP61 (SYP61-cEYFP) before being transformed into *Agrobacterium* (described in section 2.4). Positive clones for all vector transformations were selected using colony PCR and minipreps were sent for sequencing (Nanuq, Quebec) using sequencing primers listed in table 3.

2.10 Yeast complementation assay

The pYES2/CT vector is designed for expression of the protein in yeast and contains the URA3 gene for selection. A VPS51 knockout mutant in yeast was obtained

from GE healthcare (YKR020w, clone ID: 15091). UNH-pYES2/CT was transformed into the knockout VPS51 strain using the yeast transformation protocol described in section 2.5 and positive transformants were grown on SD media lacking uracil. InviSC (wild-type), YKR020w and YKR020w transformed with UNH-pYES2/CT were plated using 5-fold serial dilutions and grown on YEPD media at both 30°C and 37°C for 2-4 days.

2.11 Yeast two-hybrid histidine/3-AT and X-gal assay

To identify yeast prototrophic for histidine biosynthesis the yeast transformed with both bait and prey fusion proteins were plated onto -His, -Leu, -Trp SD supplemented with varying concentrations of 3-AT (2.5 mM, 5 mM, 10mM). Cells were grown at both 22°C and 28°C for 3-7 days to test for growth compared to a positive (AGL4-T4) and negative control (AGL4-T7 + empty bait). Simultaneously, yeast was plated on –Leu, -Trp SD plates for 3 days before testing for LacZ expression. Yeast colonies were adhered to nitrocellulose filters before being dipped into liquid nitrogen to lyse the cells. Cells were then placed cell side up on a petri dish containing filter paper soaked in Z-buffer (buffer reagents listed in appendix). Plates were incubated at 22°C and 28°C and blue coloration was assessed at regular time intervals. All fusion proteins were expressed individually in yeast for both assays to test for self-activation.

2.12 BiFC assay - tobacco injection/confocal microscopy

Tobacco seed were sown on a mixture of ¾ Flora Compo compost and ¼ vermiculite in 100 cm^2 pots. After two weeks, tobacco plants were transferred into individual pots and grown at 21°C long day conditions (16 hour light, 8 hour dark) before

infiltration of the leaves. Single colonies of *Agrobacterium* with the appropriate binary vector (pPZP-RCS2-ocs-bar-RI:pSAT1A-nEYFP:UNH, pPZP-RCS2-ocs-bar-RI:pSAT4A-cEYFP:VPS52 and pPZP-RCS2-ocs-bar-RI:pSAT4A-cEYFP:SYP61) were inoculated in LB media with the same antibiotics as above and grown overnight at 30°C. 1 mL of the culture was spun down at 4000 rpm for 5 minutes and washed twice with 1 mL infiltration buffer. The final re-suspension was diluted 5-fold, the OD_{600} was determined and the diluted suspension was then further diluted to an OD_{600} of 0.05. The inoculum was infiltrated into the lower epidermis of *Nicotiana tabacum* using a 1 mL needleless syringe. The plants were then left to grow for 48 hours before detection of EYFP on a FV1000 Olympus laser scanning confocal microscope using a 473-nm diode laser.

3. Results

3.1 *In silico* analysis of UNHINGED and putative interactors

An *in silico* approach was first initiated to better understand the role of UNHINGED in plants. I first compared the *A. thaliana* UNHINGED/VPS51 protein (UniProtKB: F4JH69) to the following orthologues whose interactions and function have been previously studied (Figure 2): *M. musculus* VPS51 (UniProtKB: Q3UVL4), *H. sapiens* Ang2/VPS51 (UniProtKB: Q9UID3), *D. rerio* VPS51/ffr (UniProtKB: Q155U0), *S. cerevisiae* VPS51/YKR020W (UniProtKB: P36116), *C. elegans* VPS51/B0414.8b (UniProtKB: G8XYY4). There was considerable similarity in the N-terminal region, but little in the remaining sequence. Since the GARP complex assembles and stabilizes using coiled-coil domains in yeast and mammalian models I analyzed whether *Arabidopsis* GARP subunits contained coiled coil structures (Liewen et al. 2005; Siniossoglou and Pelham 2002). Coiled coils are formed by two or three parallel alpha helices containing a repeated pattern of seven amino acids with the first four amino acids being generally hydrophobic (Lupas et al. 1991).

The COILS server was used to predict whether the Arabidopsis GARP subunits contained coiled-coil domains based on the known sequences of previously characterized coils (Lupas et al. 1991). Based on the 28 amino-acid window (highest probability of functionally relevant coil), UNHINGED contains two strongly predicted coils in the first 150 residues of the protein (Figure 4A). One coil overlaps with the highly conserved sequence, ‘LVYENYNKFISATDT’, found within the VPS51 domain (Figure 2A+4). Vps52/53/54 also have predicted coil domains in the first 250 residues (Figure 5). It

seems likely that the *Arabidopsis* GARP subunits, like those of yeast and humans, utilize the coiled-coil domains to assemble the complex.

SYP61, the *Arabidopsis* homologs of SYX6 and tlg1p, has been shown to co-localize with UNHINGED to punctate vesicles in *Arabidopsis* cotyledon epidermal cells (Pahari et al. 2014). In order to test whether co-localization is indicative of interaction, I looked for conserved motifs known to be responsible for interaction within VPS51 homologs. Yeast and human VPS51 interact with the H_{abc} domain of a specific t-SNARE via a short N-terminal helix containing a two amino acid motif critical for interaction (Siniossoglou and Pelham 2002). In yeast, the phenylalanine/tyrosine (PY) motif of VPS51 is required for interaction with the t-SNARE tlg1p, whereas in humans a dityrosine motif in VPS51 allows interaction with the human t-SNARE homolog, SYX6 (Siniossoglou and Pelham 2002; (Abascal-Palacios et al. 2013). Sequence comparison revealed that like yeast VPS51, UNH contains a phenylalanine/tyrosine motif (Figure 2B). Additionally, the H_{abc} domain of SYX6 has a conserved '$_{5}$DPF[…]R_{88}' motif that forms a pocket for the di-tyrosine motif to bind (Abascal-Palacios et al. 2013). Sequence comparison revealed that SYP61 and tlg1p contain a similar 'DPF[…]R' motif present in human syntaxin 6 (Stx6), suggesting a possible conserved interaction amongst Arabidopsis VPS51 and SYP61 orthologues (Figure 2C).

3.2 Complementation of UNHINGED in *vps51* yeast mutant

Although the protein sequence differs greatly between yeast and *Arabidopsis*, *in silico* analysis predicts that *Arabidopsis* UNH has domains and motifs that might form similar interactions as yeast VPS51. To assess similarity of function *in vivo,* I tested whether UNH could rescue a *vps51* knockout in yeast. UNH-pYES2/CT was transformed

into the yeast *vps51* knockout. Yeast *vps51* grows under normal conditions (30°C) but is not able to grow properly at 37°C (Figure 6), whereas wild-type grows under both conditions (Conibear et al. 2003). The yeast *vps51* knockout transformed with UNH-pYES2/CT retained the mutant phenotype: it was able to grow at 30°C but was unable to grow at 37°C (Figure 6). These results suggest that *Arabidopsis* UNH cannot carry out yeast VPS51 function.

3.3 Interactions between GARP complex members

In order to directly test whether UNH maintains conserved interactions with other *Arabidopsis* GARP complex members, a yeast two-hybrid assay was employed. The yeast two-hybrid tests interactions between proteins by utilizing the independent DNA-binding (DB) and activating (TA) domains of the GAL4 protein (Fields and Song 1989). Yeast strains are engineered to carry biochemical marker genes that are regulated by GAL4 upstream activating sequences (UAS). Proteins of interest are translationally fused to either the DB or TA domain and expressed in the YPB2 yeast strain. Interaction of the two proteins causes reconstitution of the GAL4 quaternary complex which then activates marker genes. Typical marker genes include HIS3, which allows for growth on media lacking histidine and confers resistance to 3-amino-1',2',4'-triazole (3-AT), or the LacZ reporter gene. 3-AT is a competitive inhibitor of the product of the HIS3 gene. The addition of 3-AT requires a strong protein interaction in order to generate high levels of HIS3 expression to outcompete 3-AT. 22°C was also included in order to allow protein interactions that might occur more strongly at their native temperature. In certain cases of 'self-activation', the protein that is fused to either domain can activate the HIS3 or LacZ gene on its own or can interact non-specifically with other yeast two-hybrid components

to activate the marker genes (Kohalmi et al. 1998). To ensure that expression of the marker genes is the result of protein interaction, not self-activation, each plasmid is expressed in yeast alone.

Pahari *et al* (2014) previously tested the interactions between UNH and the other 3 GARP complex members. He generated plasmids in which UNH was translationally fused to GAL4-DB and VPS52 or VPS53 was fused to GAL4-TA. As well, VPS54 was fused to GAL4-TA but the only available VPS54 cDNA unknowingly contained only the C-terminal portion (VPS54Δ552-1034aa) which does not have the predicted coiled-coil domains (Figure 5D). Pahari *et al* (2014) determined UNH interacted only with VPS52, since yeast transformed with UNH-DB and VPS52-TA activated both the HIS3 (10mM 3-AT) and LacZ genes whereas yeast transformed with UNH-DB and VPS53-TA or VPS54Δ552-1034aa-TA did not.

To test for interactions amongst other complex members, and to assess if weaker interactions might be occurring, I expanded the yeast two-hybrid by testing concentrations of 2.5 mM, 5 mM and 10 mM 3-AT in order to qualitatively assess differences in the strength of protein interactions. I generated plasmids containing VPS52, VPS53 and VPS54Δ552-1034aa translationally fused to GAL4-DB and UNHINGED fused to GAL4-TA and the fusion constructs were first tested to observe any self-activation (Figure 7-10). Yeast transformed with VPS52-DB alone grew on the -His plate supplemented with up to 10 mM 3-AT and also showed observable LacZ expression at both 22°C and 28°C (Figure 9+10). Additionally, there was slight growth detected for yeast transformed with VPS52-TA, VPS53-TA and VPS54Δ552-1034aa-TA

on the -His plates, but no LacZ expression was observed, confirming the absence of any meaningful self-interaction (Figure 7+8).

Yeast transformed with both UNH-DB and VPS52-TA grew on -His plates with up to 10 mM 3-AT concentrations and LacZ expression was observed at both 22°C and 28°C, showing a higher degree of LacZ expression at 22°C (Figure 11+12). Even under less stringent conditions (2.5 mM + 5 mM 3-AT) than tested by Pahari *et al* (2014), UNH-DB did not show any interactions with VPS53-TA or VPS54Δ552-1034aa-TA at either temperature (Figure 13+14).

Interactions amongst other GARP complex members did not activate either reporter gene. Transformation with VPS53-DB and VPS52-TA or VPS54Δ552-1034aa-TA did not result in growth on –his plates +3-AT or LacZ expression under any conditions tested (Figure 15+16). Additionally, VPS54Δ552-1034aa-DB did not show any interactions with VPS52-TA and VPS53-TA (Figure 17+18). It was surprising that VPS52 and UNH was the only interaction between any of the GARP member subunits detectable by yeast two-hybrid, though we cannot rule out the possibility that the N-terminal coils of VPS54 are the link between subunit members.

3.4 Interactions of the GARP complex with SNAREs and Rabs.

Pahari *et al* (2014) previously found no interaction between UNHINGED-DB and any of SYP22-TA, SYP41-TA, Vti11-TA or AtRab6A-TA via yeast two-hybrid. I sought to further elucidate whether different members of the GARP complex could interact with the previously tested proteins (SYP22, SYP41, Vti11, AtRab6A) at less stringent conditions as well as more likely candidate SNAREs detected via *in silico* analysis

(SYP51, SYP61, Vti12). Yeast transformed with UNHINGED-DB and both AtRab6A-TA and SYP22-TA showed slight growth at 2.5 mM, 5 mM and 10 mM 3-AT concentrations, but no observable LacZ expression at either 22°C or 28°C (Figure 13+14). It was surprising that UNHINGED-DB did not show interaction with SYP61-TA, Vti12-TA, or SYP51-TA at either temperature (Figure 13+14).

We next tested whether VPS52 could interact with SYP61 instead of the hypothesized VPS51. Due to self-activation of VPS52-DB, I could only test its interaction with SYP61 as it was the only protein fused to GAL4-DB. Yeast transformed with VPS52-TA and SYP61-DB did not grow on -His plates + 10 mM 3-AT or show LacZ expression, indicating that it does not interact with SYP61, but we cannot rule out the possibility that VPS52 interacts with other resident TGN SNAREs (Figure 19+20). Yeast transformed with VPS52-TA and AtRab6A-DB did not grow on -His plates supplemented with up to 10 mM 3-AT or show LacZ expression (Figure 19+20). VPS53-DB and VPS54Δ552-1034aa-DB showed no significant interactions with any of the proteins tested (Figure 15-18).

In order for the yeast two-hybrid assay to work, the proteins need to pass through the nuclear membrane before acting on the HIS3 or LacZ genes (Kohalmi et al. 1998). It is possible the C-terminal hydrophobic anchors of the SNAREs cause them to embed into cellular membranes, disrupting any possible interactions. We assessed whether the yeast two-hybrid could detect interaction between the TGN SYP41/SYP61/Vti12 SNARE complex previously shown via co-immunoprecipitation (Sanderfoot et al. 2001). Yeast transformed with SYP61-DB and either Vti12-TA or SYP41-TA did not grow on -His

plates supplemented with up to 10 mM 3-AT and showed no observable LacZ expression at either 22°C or 28°C (Figure 19+20).

3.5 Bimolecular Fluorescence Complementation (BiFC) assay

In order to confirm the interactions of UNHINGED and VPS52 *in planta*, a bimolecular fluorescence complementation (BiFC) assay was done. The BiFC assay utilizes a split EYFP system in which neither C-terminal nor N-terminal can fluoresce on its own. Proteins of interest are translationally fused to each EYFP half and co-transformed into *Agrobacterium* before being infiltrated into tobacco. Interacting proteins bring the two EYFP halves into proximity, allowing them to refold and restore fluorescence in tobacco epidermal cells (Lee et al. 2008). We translationally fused UNHINGED to the N-terminus of EYFP and VPS52 to the C-terminus of EYFP. Both sets of plasmids were co-transformed into tobacco leaves. Fluorescence was detected between UNH-nEYFP and VPS52-cEYFP, while no signal was detected when UNH-nEYFP or VPS52-cEYFP were expressed alone, confirming their interaction *in vivo* (Figure 21). We also tested whether VPS52-cEYFP or UNH-nEYFP could interact with the empty cEYFP and nEYFP halves. UNH-nEYFP did not show significant fluorescence when transformed with the empty cEYFP (Figure 21). Unfortunately, VPS52-cEYFP was able to fluoresce when transformed with the empty nEYFP (Figure 21). We did observe a significantly larger number of EYFP protein aggregates in tobacco epidermal cells infiltrated with VPS52-cEYFP and UNH-nEYFP compared to VPS52-cEYFP and empty n-EYFP which may indicate a stronger interaction (Figure 21).

SYP61 was not shown to interact with UNH via yeast two-hybrid. It is possible that the SYP61 transmembrane domain inhibited its transport into the nucleus, resulting

in a false-negative. A BiFC assay was utilized to observe whether they could interact *in planta.* We translationally fused UNHINGED to the N-terminus of EYFP and SYP61 to the C-terminus of EYFP. Fluorescence was not detected between UNH-nEYFP and SYP61-cEYFP, suggesting these proteins do not interact *in planta* (Figure 22).

3.6 Mutagenesis of putative domains in UNHINGED

In silico analysis of UNH revealed key regions of interest. In order to determine which domains of UNHINGED are important for interaction with VPS52, 4 truncated versions were created and translationally fused to the DB of pbi-770.

The UNH N-terminal region is predicted to form two coiled-coil structures (50-85 aa and 95-130 aa; Figure 4A). Both predicted coiled-coils partially overlap with the VPS51 domain. The second predicted coiled-coil completely overlaps with the high sequence similarity motif 'LVYENYNKFISATDT' (Figure 2A). In order to determine which of the two coiled-coils were important, two truncated mutants of UNH were created. UNHΔ1-118aa was created in order to observe whether the predicted 50-78aa coiled-coil alone was sufficient for interaction as it disrupts the second coiled coil only (Figure 4B). UNHΔ78-780 aa was made to include the entire protein without the predicted 50-78 aa coiled-coil, but including the second coiled-coil containing the highly conserved VPS51 motif (Figure 4D).

UNH is also predicted to contain three small coiled-coils at position 203-290 aa (Figure 4A). UNHΔ1-289 aa was created to include all predicted coiled-coil structures without the C-terminal region (Figure 4C). The C-terminal region has low sequence similarity between VPS51 homologs with no predicted coiled-coil structures (291-780 aa;

Figure 2A). UNHΔ291-780 aa was designed to observe whether the C-terminal region could interact with VPS52 without any predicted coiled-coil structures (Figure 4E). Sequencing revealed that UNH Primer_ATW_leftborder_Fwd3 amplified in an incorrect location instead resulting in a shortened C-terminal truncated mutant UNHΔ586-780 aa.

Yeast transformed with UNHΔ1-118 aa-DB and VPS52-TA showed reduced growth on all 3-AT concentrations as well as a marked reduction in LacZ expression, though it was not completely abolished (Figure 11+12). It is also interesting to note that there was a stronger interaction between UNHΔ1-118 aa-DB and VPS52-TA at 22°C, which may be due to proteins folding better at their native temperatures (Figure 11+12). Yeast transformed with UNHΔ78-780 aa-DB and VPS52-TA showed a slight reduction compared to UNH-DB. LacZ and histidine expression were fully restored at all temperatures and 3-AT concentrations tested when UNHΔ1-289 aa-DB was transformed with VPS52-TA. The C-terminal mutant UNHΔ586-780 aa-DB was not able to activate either the LacZ or HIS3 gene when transformed with VPS52-TA (Figure 11+12).

4. Discussion

The GARP complex is present in all eukaryotes analyzed and functions in controlling retrograde vesicle transport from the endosome to the late Golgi/TGN (Whyte and Munro 2002). Since the GARP complex functions in an evolutionary conserved manner, I hypothesized that the Arabidopsis homolog of VPS51 (UNHINGED) as well as the other GARP subunits will interact with conserved domains and share conserved motifs important for those interactions.

4.1 UNH interacts with VPS52 via N-terminal coiled-coil domains.

In both yeast and mammalian systems the GARP complex subunits are shown to interact with each other via their N-terminal coiled-coil domains (Liewen et al. 2005; Siniossoglou and Pelham 2002). A coiled-coil prediction program revealed that all *Arabidopsis* GARP subunits contain highly predicted N-terminal coiled coil domains. In order to test the validity of these interactions, yeast two-hybrid assays were performed.

Yeast two-hybrid analysis revealed that of the interactions tested, only VPS51 interacted with VPS52, as shown by Pahari *et al* (2014). In order to confirm the yeast two-hybrid interactions, VPS52-cEYFP and UNHINGED-nEYFP were expressed *in planta* using a bimolecular fluorescence complementation assay. Unfortunately, VPS52-cEYFP could interact with nEYFP alone so the apparent *in planta* interaction of UNH and VPS52 is questionable. However, the cells expressing VPS52-cEYFP and UNH-nEYFP display large aggregates of EYFP as compared to VPS52-cEYFP with the empty nEYFP suggesting a stronger interaction.

In order to elucidate the domains of UNH required for interaction with VPS52, deletional mutagenesis was done. *In silico* analysis revealed that UNHINGED contains several potential domains important for interaction: an N-terminal VPS51 domain (80-165 aa), several potential coiled-coil domains (50-78 aa, 95-130 aa, 250-278 aa) and a phenylalanine/tyrosine motif. The C-terminal domain contains no predicted coiled-coils and has little sequence similarity to the other VPS51 proteins. Four different mutants were constructed and tested for interaction within the yeast two-hybrid to observe which domains/motifs are important for interaction. UNHΔ1-118aa was created in order to observe whether the predicted 50-78 aa coiled-coil alone was sufficient for interaction. UNHΔ78-780 aa was made to include the entire protein without the predicted 50-78 aa coiled-coil, but including the second coiled-coil containing the highly conserved VPS51 motif. UNHΔ1-289 aa was created to include all predicted coiled-coil structures while UNHΔ291-780 aa was made to observe whether the C-terminal region could interact without any predicted coiled-coil structures.

UNHΔ78-780 aa contains the predicted coiled-coil that overlaps with the highly conserved sequence motif and was shown to interact with VPS52 via yeast two-hybrid, though the interaction was slightly less intense compared to the full length UNH. Yeast expressing both UNHΔ1-118 aa and VPS52 showed considerably less growth on –his + 3-AT plates and a slight reduction in LacZ expression. This would suggest that the second predicted coiled-coil structure (95-130 aa) is more important for interaction with VPS52. The VPS51 domain is a broad region of sequence similarity, with UNH showing sequence similarity within its highly conserved sequence 'LVYENYNKFISATDT' motif only. Interestingly, this sequence motif forms part of the 95-130 aa predicted coil,

suggesting the evolutionary conservation of this region is due to a critical role in the VPS51/VPS52 interaction. UNHΔ1-289 aa contains all the predicted coiled coils and was able to fully interact with VPS52 via the yeast two-hybrid. It appears that both coils, not just the conserved region, form the most stable VPS51/VPS52 interaction. UNHΔ586-780 aa was not able to interact with VPS52, supporting the hypothesis that the N-terminal coils are necessary for interaction.

4.2 Yeast two-hybrid assays revealed no interactions amongst VPS52, VPS53 or the C terminus of VPS54.

I performed yeast two-hybrid assays at lower stringencies and different temperatures in order to observe possible weaker interactions between GARP complex members. UNH was not able to interact with VPS53 or VPS54Δ552-1034 aa and VPS52 did not interact with VPS53 or VPS54Δ552-1034 aa, even at the lowest stringency tested. In humans, the coiled-coil domains of VPS53 and VPS54 combine to form an extended coil that is important for interaction with certain SNARE proteins (Pérez-Victoria and Bonifacino 2009). It is possible that VPS53 and VPS54 are both required for GARP complex formation in *Arabidopsis* before VPS52 or UNHINGED can interact with VPS53 or VPS54. VPS54Δ552-1034 aa lacks the predicted coiled-coil domains thought to be involved in GARP subunit interaction, most likely hampering its ability to interact.

4.3 GARP interactions with other vesicle transport proteins

In yeast, VPS51 and the H_{abc} domain of the SNARE tlg1p are shown to interact (Figure 1)(Siniossoglou et al. 2000). The presence of the phenylalanine/tyrosine motif in *Arabidopsis* VPS51 suggests it may interact with SNAREs in a similar manner to yeast

(Figure 1). Complementation analysis revealed that *Arabidopsis* VPS51 was not able to rescue the yeast VPS51 knockout mutant. Yeast has a very small VPS51 subunit (164 amino acids) compared to mammalian and plant homologs. Additionally, although it does have the Phe/Tyr motif, yeast does not contain the conserved 'LVYENYNKFISATDT' sequence motif. It is probable that UNHINGED has diversified sufficiently to evolve unique interactions or novel functions that are not similar in the yeast system. In order to better understand how the GARP complex achieves tethering in plants, AtRab6a and the SNAREs associated with either the TGN (SYP41/51/61/Vti12) or PVC/MVB (SYP22/Vti11/SYP51) were tested via yeast two-hybrid for interaction with all GARP complex subunits (VPS54Δ552-1034 aa). Surprisingly, there were no confirmed interactions with any of the GARP subunits.

4.4 Problems and Future Directions

Using yeast two hybrid assays, this study failed to detect interactions between Arabidopsis GARP complex proteins and SNARE tethers or RAB regulators that have been observed in other organisms. The yeast two-hybrid is a relatively easy to use assay that allows for detection of protein interactions, but it does come with certain drawbacks. A key requirement for the yeast two-hybrid to work is that the expressed protein fusions must be transported to the nucleus. If the transport is impeded it will lead to false negatives (Bruckner et al. 2009). False negatives can also occur due to a lack of post translational modification when expressing proteins of higher eukaryotes (Bruckner et al. 2009). Most SNARE proteins contain a C-terminal hydrophobic membrane anchor for localization within the cell. When the SNARE protein fusions are translated in the yeast cytoplasm, they must localize to the nucleus in order to activate transcription of the

reporter gene. It is possible the hydrophobic membrane anchor causes the SNAREs to embed in the cellular membrane, disrupting HIS3 or LacZ gene activation. Co-immunoprecipitation confirmed that SYP41/61/Vti12 form a Q_{abc} complex (Sanderfoot et al. 2001). SYP41/61/vti12 were also tested within the yeast two-hybrid assay to observe whether the interactions could be detected. Using the yeast two hybrid assay, I was unable to detect interaction between SYP61 and either SYP41 or vti12. Though the co-immunoprecipitation interaction may be artificial, this suggests a possible problem within the yeast two-hybrid. In a similar yeast two hybrid assay, Heese *et al* (2001) expressed the C-terminal KNOLLE SNARE protein (lacking its trans-membrane domain) and the truncated protein was able to interact with three different SNAP proteins (Heese et al. 2001). In order to test whether the trans-membrane domain (TMD) is the problem, removal of the TMDs from SYP41, SYP61 and VTI12 via deletional mutagenesis would be necessary.

Yeast ypt6 has been shown previously to interact with VPS52 via GST pull-down assays (Siniossoglou and Pelham 2002). The *Arabidopsis* ypt6 homolog, AtRab6A, was not shown to interact with VPS52 via yeast two-hybrid. Both AtRab6A and Ypt6 contain the CxC motif that undergoes post-translational prenylation of a geranylgeranyl group which embeds it into the correct membrane (Zhang and Casey 1996). The conserved CxC motif suggest AtRab6A might also undergo prenylation in yeast and could possibly embed into the membrane, resulting in a false-negative yeast two-hybrid result. It would be interesting to observe whether removal of the CxC motif would result in a positive interaction in further yeast two-hybrid assays.

The bimolecular complementation assay allows for the detection of protein interactions *in planta*, and is not limited by membrane domains or problems with post translational modifications when expressing plant proteins. However, the BiFC does come with certain drawbacks that may result in either false negatives or false positives. The YFP protein is prone to reconstitute in the absence of any protein interaction, leading to high levels of background fluorescence (Lee et al. 2008). An endogenous low level promoter is typically used to avoid high levels of background fluorescence. The construct used in this study was controlled by a very strong double 35S CaMV promoter. It is possible the background signal observed in the VPS52-cEYFP + empty-nEYFP was due to over-expression and nonspecific YFP association (Walter et al. 2004). Both Martin *et al* (2009) and Citovsky *et al* (2006) have previously shown that the double 35S CaMV promoter construct is capable of detecting only significant protein interactions with limited background fluorescence, so it is not clear whether non-specific interaction is the problem. In future, mutations to the coiled coils of UNH or VPS52 should be introduced and compared to the wild-type. A significant reduction in protein aggregates in the mutated protein would lend support to the significance of the VPS52 and UNH interaction.

False negatives may occur due to steric hindrance if the proteins of interest separate the halves of the YFP and do not allow them to reconstitute. Steric hindrance is typically observed when the proteins are associated into large complexes (Walter et al. 2004). It could that the GARP complex interacts with the SYP41/SYP61/Vti12 SNARE complex, but the interaction separates the SYP61 and UNH proteins, resulting in the YFP halves not being able to reconstitute into a functional protein. Additionally, it is unknown

whether the N-terminal or C-terminal region of UNH and SYP61 is necessary for interaction. The EYFP protein could inhibit the interaction depending on which end it is fused to. To test for this possibility EYFP should be fused to the C-terminal and N-terminal portion of UNH and SYP61.

No interaction between the GARP complex members and other proteins associated with vesicle transport was revealed by yeast two-hybrid and BiFC binary assays. In order to screen a larger number of putative interactions a different set of experiments should be utilized. For example, initiating a bait BiFC would be useful to screen a large number of proteins simultaneously. Any of the GARP complex subunits could be fused to nEYFP and an *Arabidopsis* cDNA library could be fused to cEYFP (Lee et al. 2012). Screening for fluorescence in *Arabidopsis* protoplasts may reveal novel protein interactions. It is also possible that the full length VPS54 protein provides the bridge between the core GARP complex subunits. Additionally, it may interact with some the SNAREs or Rabs tested. Initiating a yeast two-hybrid with the full length VPS54 is necessary to completely assess the yeast two-hybrid GARP complex interactions. Other methods could also be employed to test interactions *in vitro* such as co-immunoprecipitation, pull-down assays and mass spectrometry.

5. Conclusions

This thesis used a combination of *in silico* analysis, yeast-two hybrid assays, deletional mutagenesis and bimolecular fluorescence complementation assays in order to; 1) elucidate the role of the GARP complex subunits in *Arabidopsis thaliana*, and 2) analyze which domains of UNH/VPS51 were important for interaction with VPS52.

In silico analysis revealed that *Arabidopsis* GARP complex subunits contained conserved coiled-coil structures within the N-terminal region that are important for the assembly and stabilization in other organisms. Apart from theVPS52 and UNH interaction, the yeast two-hybrid assays could not verify any interactions between the subunits tested, though the full length VPS54 remains to be tested and may provide the link between the other subunits. A BiFC assay was utilized to confirm the *in planta* interaction of UNH and VPS52, but VPS52-cEYFP interacts with empty-nEYFP, leading to an inconclusive result. A combination of deletional mutagenesis and yeast two-hybrid assays revealed that UNH contains a two highly predicted coiled-coils, one of which overlaps with an evolutionary conserved sequence, and this coil is the most critical for interaction with VPS52.

None of the GARP complex subunits were able to interact via yeast two-hybrid with a variety of TGN and PVC SNAREs and the Rab GTPases, AtRab6A. There is a possibility of a false-negative due to inherent problems within the yeast two-hybrid so we cannot rule out the possibility that the GARP complex interacts with the SNARE and Rab proteins

References

Abascal-Palacios G, Schindler C, Rojas Adriana L, Bonifacino Juan S, Hierro A (2013) Structural Basis for the Interaction of the Golgi-Associated Retrograde Protein Complex with the t-SNARE Syntaxin 6. Structure 21 (9):1698-1706.

Alberts B, Johnson A, Lewis J, Raff M, Roberts K, Walter P (2002) Intracellular compartments and protein sorting.

Bednarek SY, Reynolds TL, Schroeder M, Grabowski R, Hengst L, Gallwitz D, Raikhel NV (1994) A small GTP-binding protein from Arabidopsis thaliana functionally complements the yeast YPT6 null mutant. Plant physiology 104 (2):591-596

Bock JB, Matern HT, Peden AA, Scheller RH (2001) A genomic perspective on membrane compartment organization. Nature 409 (6822):839-841

Boevink P, Oparka K, Cruz SS, Martin B, Betteridge A, Hawes C (1998) Stacks on tracks: the plant Golgi apparatus traffics on an actin/ER network†. The Plant Journal 15 (3):441-447

Brandizzi F, Wasteneys GO (2013) Cytoskeleton-dependent endomembrane organization in plant cells: an emerging role for microtubules. The Plant Journal 75 (2):339-349.

Brennwald P, Kearns B, Champion K, Keränen S, Bankaitis V, Novick P (1994) Sec9 is a SNAP-25-like component of a yeast SNARE complex that may be the effector of Sec4 function in exocytosis. Cell 79 (2):245-258

Cai H, Reinisch K, Ferro-Novick S (2007) Coats, tethers, Rabs, and SNAREs work together to mediate the intracellular destination of a transport vesicle. Developmental cell 12 (5):671-682

Clary DO, Griff IC, Rothman JE (1990) SNAPs, a family of NSF attachment proteins involved in intracellular membrane fusion in animals and yeast. Cell 61 (4):709-721

Conibear E, Cleck JN, Stevens TH (2003) Vps51p Mediates the Association of the GARP (Vps52/53/54) Complex with the Late Golgi t-SNARE Tlg1p. Molecular Biology of the Cell 14 (4):1610-1623.

Conibear E, Stevens TH (2000) Vps52p, Vps53p, and Vps54p form a novel multisubunit complex required for protein sorting at the yeast late Golgi. Molecular Biology of the Cell 11 (1):305-323

Contento AL, Bassham DC (2012) Structure and function of endosomes in plant cells. Journal of cell science 125 (15):3511-3518

Cooper GM (2000) The Cell: A Molecular Approach. ASM Press,

Citovsky, Vitaly, Lan-Ying Lee, Shachi Vyas, Efrat Glick, Min-Huei Chen, Alexander Vainstein, Yedidya Gafni, Stanton B. Gelvin, and Tzvi Tzfira. "Subcellular localization of interacting proteins by bimolecular fluorescence complementation in planta." Journal of molecular biology 362, no. 5 (2006): 1120-1131.

Demircioglu FE, Burkhardt P, Fasshauer D (2014) The SM protein Sly1 accelerates assembly of the ER–Golgi SNARE complex. Proceedings of the National Academy of Sciences 111 (38):13828-13833

Dettmer J, Friml J (2011) Cell polarity in plants: when two do the same, it is not the same. Current opinion in cell biology 23 (6):686-696

Dettmer J, Hong-Hermesdorf A, Stierhof Y-D, Schumacher K (2006) Vacuolar H+-ATPase activity is required for endocytic and secretory trafficking in Arabidopsis. The Plant Cell 18 (3):715-730

Fasshauer D, Antonin W, Subramaniam V, Jahn R (2002) SNARE assembly and disassembly exhibit a pronounced hysteresis. Nature Structural & Molecular Biology 9 (2):144-151

Fernandez I, Ubach J, Dulubova I, Zhang X, Südhof TC, Rizo J (1998) Three-dimensional structure of an evolutionarily conserved N-terminal domain of syntaxin 1A. Cell 94 (6):841-849

Fiebig KM, Rice LM, Pollock E, Brunger AT (1999) Folding intermediates of SNARE complex assembly. Nature structural & molecular biology 6 (2):117-123

Fields S, Song O-k (1989) A novel genetic system to detect protein protein interactions.

Fridmann-Sirkis Y, Kent HM, Lewis MJ, Evans PR, Pelham HRB (2006) Structural Analysis of the Interaction Between the SNARE Tlg1 and Vps51. Traffic 7 (2):182-190.

Furgason ML, MacDonald C, Shanks SG, Ryder SP, Bryant NJ, Munson M (2009) The N-terminal peptide of the syntaxin Tlg2p modulates binding of its closed conformation to Vps45p. Proceedings of the National Academy of Sciences 106 (34):14303-14308

Glick BS, Rothman JE (1987) Possible role for fatty acyl-coenzyme A in intracellular protein transport.

Gu F, Crump CM, Thomas G (2001) Trans-Golgi network sorting. Cellular and molecular life sciences : CMLS 58 (8):1067-1084

Guermonprez H, Smertenko A, Crosnier M-T, Durandet M, Vrielynck N, Guerche P, Hussey PJ, Satiat-Jeunemaitre B, Bonhomme S (2008) The POK/AtVPS52 protein localizes to several distinct post-Golgi compartments in sporophytic and gametophytic cells. Journal of Experimental Botany 59 (11):3087-3098.

Hála M, Cole R, Synek L, Drdová E, Pečenková T, Nordheim A, Lamkemeyer T, Madlung J, Hochholdinger F, Fowler JE (2008) An exocyst complex functions in plant cell growth in Arabidopsis and tobacco. The Plant Cell Online 20 (5):1330-1345

Hawes C, Satiat-Jeunemaitre B (2005) The plant Golgi apparatus—going with the flow. Biochimica et Biophysica Acta (BBA)-Molecular Cell Research 1744 (2):93-107

He B, Xi F, Zhang J, TerBush D, Zhang X, Guo W (2007) Exo70p mediates the secretion of specific exocytic vesicles at early stages of the cell cycle for polarized cell growth. The Journal of cell biology 176 (6):771-777

Heese M, Gansel X, Sticher L, Wick P, Grebe M, Granier F, Jürgens G (2001) Functional characterization of the KNOLLE-interacting t-SNARE AtSNAP33 and its role in plant cytokinesis. The Journal of Cell Biology 155 (2):239-250.

Herman EM, Larkins BA (1999) Protein storage bodies and vacuoles. The Plant Cell 11 (4):601-613

Hutagalung AH, Novick PJ (2011) Role of Rab GTPases in Membrane Traffic and Cell Physiology, vol 91. vol 1.

Kohalmi SE, Reader LJ, Samach A, Nowak J, Haughn GW, Crosby WL (1998) Identification and characterization of protein interactions using the yeast 2-hybrid system. In: Plant molecular biology manual. Springer, pp 95-124

Lam SK, Tse YC, Robinson DG, Jiang L (2007) Tracking down the elusive early endosome. Trends in plant science 12 (11):497-505

Lee C-F, Pu H-Y, Wang L-C, Sayler RJ, Yeh C-H, Wu S-J (2006) Mutation in a homolog of yeast Vps53p accounts for the heat and osmotic hypersensitive phenotypes in Arabidopsis hit1-1 mutant. Planta 224 (2):330-338

Lee L-Y, Fang M-J, Kuang L-Y, Gelvin SB (2008) Vectors for multi-color bimolecular fluorescence complementation to investigate protein-protein interactions in living plant cells. Plant Methods 4 (1):1-11

Li H, Lin Y, Heath RM, Zhu MX, Yang Z (1999) Control of pollen tube tip growth by a Rop GTPase–dependent pathway that leads to tip-localized calcium influx. The Plant Cell 11 (9):1731-1742

Liewen H, Meinhold-Heerlein I, Oliveira V, Schwarzenbacher R, Luo G, Wadle A, Jung M, Pfreundschuh M, Stenner-Liewen F (2005) Characterization of the human GARP (Golgi associated retrograde protein) complex. Experimental Cell Research 306 (1):24-34.

Lipka V, Kwon C, Panstruga R (2007) SNARE-Ware: The Role of SNARE-Domain Proteins in Plant Biology. Annual Review of Cell and Developmental Biology 23 (1):147-174.

Luo L, Hannemann M, Koenig S, Hegermann J, Ailion M, Cho M-K, Sasidharan N, Zweckstetter M, Rensing SA, Eimer S (2011) The Caenorhabditis elegans GARP complex contains the conserved Vps51 subunit and is required to maintain lysosomal morphology. Molecular Biology of the Cell 22 (14):2564-2578.

Lupas A, Van Dyke M, Stock J (1991) Predicting coiled coils from protein sequences. Science 252 (5009):1162-1164

Malhotra V, Orci L, Glick BS, Block MR, Rothman JE (1988) Role of an N-ethylmaleimide-sensitive transport component in promoting fusion of transport vesicles with cisternae of the Golgi stack. Cell 54 (2):221-227

Martin, K., Kopperud, K., Chakrabarty, R., Banerjee, R., Brooks, R. and Goodin, M. M. (2009), Transient expression in *Nicotiana benthamiana* fluorescent marker lines provides enhanced definition of protein localization, movement and interactions *in planta*. The Plant Journal, 59: 150–162.

Marty F (1999) Plant vacuoles. The Plant Cell Online 11 (4):587-599

Monier S, Jollivet F, Janoueix-Lerosey I, Johannes L, Goud B (2002) Characterization of Novel Rab6-Interacting Proteins Involved in Endosome-to-TGN Transport. Traffic 3 (4):289-297.

Novick P, Guo W (2002) Ras family therapy: Rab, Rho and Ral talk to the exocyst. Trends in cell biology 12 (6):247-249

Pahari S, Cormark RD, Blackshaw MT, Liu C, Erickson JL, Schultz EA (2014) Arabidopsis UNHINGED encodes a VPS51 homolog and reveals a role for the GARP complex in leaf shape and vein patterning. Development 141 (9):1894-1905

Pečenková T, Hála M, Kulich I, Kocourková D, Drdová E, Fendrych M, Hana T, Žárský V (2011) The role for the exocyst complex subunits Exo70B2 and Exo70H1 in the plant–pathogen interaction. Journal of experimental botany:erq402

Pedrazzini E, Komarova NY, Rentsch D, Vitale A (2013) Traffic routes and signals for the tonoplast. Traffic 14 (6):622-628

Pereira-Leal JB, Seabra MC (2000) The mammalian Rab family of small GTPases: definition of family and subfamily sequence motifs suggests a mechanism for functional specificity in the Ras superfamily. Journal of molecular biology 301 (4):1077-1087

Pereira-Leal JB, Seabra MC (2001) Evolution of the Rab family of small GTP-binding proteins. Journal of molecular biology 313 (4):889-901

Pérez-Victoria FJ, Bonifacino JS (2009) Dual Roles of the Mammalian GARP Complex in Tethering and SNARE Complex Assembly at the trans-Golgi Network. Molecular and Cellular Biology 29 (19):5251-5263.

Pérez-Victoria FJ, Mardones GA, Bonifacino JS (2008) Requirement of the human GARP complex for mannose 6-phosphate-receptor-dependent sorting of cathepsin D to lysosomes. Molecular biology of the cell 19 (6):2350-2362

Pérez-Victoria FJ, Schindler C, Magadán JG, Mardones GA, Delevoye C, Romao M, Raposo G, Bonifacino JS (2010) Ang2/Fat-Free Is a Conserved Subunit of the Golgi-associated Retrograde Protein Complex. Molecular Biology of the Cell 21 (19):3386-3395.

Pfeffer SR (1996) Transport vesicle docking: SNAREs and associates. Annual review of cell and developmental biology 12 (1):441-461

Presley JF, Cole NB, Schroer TA, Hirschberg K, Zaal KJ, Lippincott-Schwartz J (1997) ER-to-Golgi transport visualized in living cells. Nature 389 (6646):81-85

Quenneville NR, Chao T-Y, McCaffery JM, Conibear E (2006) Domains within the GARP Subunit Vps54 Confer Separate Functions in Complex Assembly and Early Endosome Recognition. Molecular Biology of the Cell 17 (4):1859-1870.

Rothman JE (1994) Mechanisms of intracellular protein transport.

Rutherford S, Moore I (2002) The Arabidopsis Rab GTPase family: another enigma variation. Current opinion in plant biology 5 (6):518-528

Sachs T (1981) The Control of the Patterned Differentiation of Vascular Tissues. In: Woolhouse HW (ed) Advances in Botanical Research, vol Volume 9. Academic Press, pp 151-262.

Sanderfoot AA, Assaad FF, Raikhel NV (2000) The Arabidopsis Genome. An Abundance of Soluble N-Ethylmaleimide-Sensitive Factor Adaptor Protein Receptors. Plant Physiology 124 (4):1558-1569.

Sanderfoot AA, Kovaleva V, Bassham DC, Raikhel NV (2001) Interactions between Syntaxins Identify at Least Five SNARE Complexes within the Golgi/Prevacuolar System of the Arabidopsis Cell. Molecular Biology of the Cell 12 (12):3733-3743.

Schmitt-John T, Drepper C, Mußmann A, Hahn P, Kuhlmann M, Thiel C, Hafner M, Lengeling A, Heimann P, Jones JM (2005) Mutation of Vps54 causes motor neuron disease and defective spermiogenesis in the wobbler mouse. Nature genetics 37 (11)

Siniossoglou S, Peak-Chew SY, Pelham HR (2000) Ric1p and Rgp1p form a complex that catalyses nucleotide exchange on Ypt6p. The EMBO Journal 19 (18):4885-4894

Siniossoglou S, Pelham HRB (2001) An effector of Ypt6p binds the SNARE Tlg1p and mediates selective fusion of vesicles with late Golgi membranes. The EMBO Journal 20 (21):5991-5998.

Siniossoglou S, Pelham HRB (2002) Vps51p Links the VFT Complex to the SNARE Tlg1p. Journal of Biological Chemistry 277 (50):48318-48324.

Söllner T, Whiteheart SW, Brunner M, Erdjument-Bromage H, Geromanos S, Tempst P, Rothman JE (1993) SNAP receptors implicated in vesicle targeting and fusion. Nature (362):318-324

Sutton RB, Fasshauer D, Jahn R, Brunger AT (1998) Crystal structure of a SNARE complex involved in synaptic exocytosis at 2.4 Å resolution. Nature 395 (6700):347-353

Suvorova E, Lupashin V COG complex interacts with the components of the Golgi tethering machinery. In: MOLECULAR BIOLOGY OF THE CELL, 2002. AMER SOC CELL BIOLOGY 8120 WOODMONT AVE, STE 750, BETHESDA, MD 20814-2755 USA, pp 266A-266A

Tahirovic S, Bradke F (2009) Neuronal polarity. Cold Spring Harbor perspectives in biology 1 (3):a001644

Takai Y, Sasaki T, Matozaki T (2001) Small GTP-Binding Proteins, vol 81. vol 1.

Uemura T, Ueda T, Ohniwa RL, Nakano A, Takeyasu K, Sato MH (2004) Systematic analysis of SNARE molecules in Arabidopsis: dissection of the post-Golgi network in plant cells. Cell structure and function 29 (2):49-65

Vernoud V, Horton AC, Yang Z, Nielsen E (2003) Analysis of the small GTPase gene superfamily of Arabidopsis. Plant physiology 131 (3):1191-1208

Viotti C, Bubeck J, Stierhof Y-D, Krebs M, Langhans M, van den Berg W, van Dongen W, Richter S, Geldner N, Takano J (2010) Endocytic and secretory traffic in Arabidopsis merge in the trans-Golgi network/early endosome, an independent and highly dynamic organelle. The Plant Cell 22 (4):1344-1357

Vitale A, Raikhel NV (1999) What do proteins need to reach different vacuoles? Trends in plant science 4 (4):149-155

Wang L-C, Tsai M-C, Chang K-Y, Fan Y-S, Yeh C-H, Wu S-J (2011) Involvement of the Arabidopsis HIT1/AtVPS53 tethering protein homologue in the acclimation of the plasma membrane to heat stress. Journal of Experimental Botany 62 (10):3609-3620.

Whyte JR, Munro S (2001) The Sec34/35 Golgi transport complex is related to the exocyst, defining a family of complexes involved in multiple steps of membrane traffic. Developmental cell 1 (4):527-537

Whyte JR, Munro S (2002) Vesicle tethering complexes in membrane traffic. Journal of Cell Science 115 (13):2627-2637

Willett R, Ungar D, Lupashin V (2013) The Golgi puppet master: COG complex at center stage of membrane trafficking interactions. Histochemistry and cell biology 140 (3):271-283

Woollard AA, Moore I (2008) The functions of Rab GTPases in plant membrane traffic. Current opinion in plant biology 11 (6):610-619

Wuestehube LJ, Duden R, Eun A, Hamamoto S, Korn P, Ram R, Schekman R (1996) New mutants of Saccharomyces cerevisiae affected in the transport of proteins from the endoplasmic reticulum to the Golgi complex. Genetics 142 (2):393

Ye J, Coulouris G, Zaretskaya I, Cutcutache I, Rozen S, Madden TL (2012) Primer-BLAST: a tool to design target-specific primers for polymerase chain reaction. BMC bioinformatics 13 (1):134

Yeaman C, Grindstaff KK, Nelson WJ (1999) New perspectives on mechanisms involved in generating epithelial cell polarity. Physiological reviews 79 (1):73-98

Zhang FL, Casey PJ (1996) Protein Prenylation: Molecular Mechanisms and Functional Consequences. Annual Review of Biochemistry 65 (1):241-269.

Zhang Y, Liu CM, Emons AMC, Ketelaar T (2010) The plant exocyst. Journal of integrative plant biology 52 (2):138-146

Zhao Y (2010) Auxin biosynthesis and its role in plant development. Annual review of plant biology 61:49-64. doi:10.1146/annurev-arplant-042809-112308

Table 1. cDNA amplification primers for constructs. Restriction cut sites are underlined for relevant primers, melting temperatures (T_m) are for annealing portions under standard concentrations listed in section 2.8.

Primer Name	Sequence (5' to 3')	T_m (C)	Extension Time (min:sec)	Enzyme
UNH_pYES_KpnI_F	ATTAGGTACCCAAACAATGTCCGCGACGGAGGCAGCTC	65	1:30	KpnI
UNH_pYES_EcoRI_R	TATAGAATTCACTACGGATGATAACAAGAAGCGG	64.4		EcoRI
SYP51_pbi_fwd2	GAGTCGACGGATGGCGTCTTCATCGGTAAC	62.4	0:30	SalI
Syp51_pbi_not_R	AAAGCGGCCGCTTACATATACTTAACC	43		NotI
VTI12_pbi771_F	GAGAGTCGACGGATGTCCGTGGAGAGGCT	62.6	0:15	SalI
VTI12_pbi771_R	AAAGCGGCCGCTTAATGAGAAAGCTTGT	51		NotI
SYP41_PBI_F	GAGAGTCGACGGATGGCGACGAGGAATCG	61.6	0:30	SalI
SYP41_PBI_R	AAAGCGGCCGCTCACAAGAATATTTCCT	50		NotI
SYP61_PBI_F	GAGAGTCGACGGATGTCTTCAGCTCAAGAT	55.9	0:30	SalI
SYP61_PBI_R	AAAGCGGCCGCTTAGGTCAAGAAGAC	47.9		NotI
Primer_ATW_leftborder_NewRev2	CATTTTTCTAAACTCCTGCTTC	48.7		
Primer_ATW_leftborder_Fwd1	CTCGACACAGACTTGCAA	58.2	3:00	
Primer_ATW_leftborder_Fwd2	ATGGAAGGCAATATGGACC	59.8	3:00	
Primer_ATW_leftborder_Fwd3	AGCAATGACCAACATCCT	59.2	2:30	
Primer_ATW_rightborder_Fwd	AGTTGAGGACGAAGCTGC	62.1		
Primer_ATW_rightborder_rev4	TTAAATCTCAGCAGCCATTTGAAC	61.6	2:00	
Primer_ATW_rightborder_rev5	TTACTGGTCCATATTGCCTTCCAT	62.4	2:00	
Primer_ATW_rightborder_rev6	TTAAGGATGTTGGTCATTGCTTTC	61.4	2:30	
UNH_pSAT_SalI _F	ATATGTCGACGAGTTTAGAAAAATGCG	51.1	1:30	SalI
UNH_pSAT_KpnI_R	ATTAGGTACCAAGAAGAAACTGTGTTGT	54.7		KpnI
VPS52_pSAT_SalI _F	ATTAGTCGACAATCTCATTAGGAAGATGTCC	57.4	1:30	SalI
VPS52_pSAT_KpnI_R	ATTAGGTACCAGAAAGTCTTGGAGTATTTCC	57.8		KpnI
SYP61_pSAT_SalI _F	ATTAGTCGACATGTCTTCAGCTCAAGATC	57.1	0:30	SalI
SYP61_pSAT_KpnI_R	TAATGGTACCTCAAGAAGACAAGAACGAAT	57.6		KpnI

Table 2. Primers used for sequencing submissions and colony PCR. Sequencing primer melting temperatures (T_m) are for annealing portions under standard concentrations listed in section 2.8.

Primer Name	Sequence (5' to 3')	T_m (C)	Vector/cDNA
pYES2CT_sequencing_F	AAT ATA CCT CTA TAC TTT AAC GTC	56.9	pYES2/CT
pYES2CT_sequencing_R	ATC GGC GAA AGG ATA TGG	60	pYES2/CT
UNHcDNA_Seq_R1	AAA AGA GAA GTG TTG ACC CC	61	UNHINGED
UNHcDNA_Seq_F2	GGA AGG CAA TAT GGA CCA GC	63.7	UNHINGED
UNHcDNA_Seq_R2	TGG TCA TTG CTT TCT GTA TCG T	63.2	UNHINGED
UNHcDNA_Seq_F3	AGC CTG AGG AGG CAA GTA CA	66	UNHINGED
UNHcDNA_Seq_R3	CCT TTC TGA ATC CAA CCA CTG A	63.3	UNHINGED
UNHcDNA_Seq_F4	AGT GCT ACA AGG CAC CAC AA	65.2	UNHINGED
UNHcDNA_Seq_R4	TGT GCT TAC GGA AAG TCC CT	64.4	UNHINGED
UNHcDNA_Seq_F5	TCA CGA GTT AGA AGA AGT TGG	60.5	UNHINGED
SYP51_primerF_sequencing	ATC GGC GAA AGG ATA TGG	60	SYP51
SYP51_primerR_sequencing	GAG CAA GCT GTC TCT ATT G	58.6	SYP51
Syp71_pbi_seq_F	CTC AAC AAC ATC TCG TCC TG	61.1	SYP71
Syp71_pbi_seq_R	GTA ATC ATC GTC AAA ACG CC	60.4	SYP71
Syp61_pbi_seq_F	GGA ATG TGA AGT CTG GTG TT	61.1	SYP61
Syp61_pbi_seq_r	GTT CTC TAC GCA CTT CAC TT	60.6	SYP61
BC293	GAATAAGTGCGACATCATC	56.9	Pbi-770
BC304	CTATTCGATGATGAAGATACC	56.5	Pbi-771
JN069	TTGATTGGAGACTTGACC	57.5	Pbi771+Pbi770
pJET1.2 Forward Sequencing Primer	CGACTCACTATAGGGAGAGCGGC	67.7	pJET1.2
pJET1.2 Reverse Sequencing Primer	AAGAACATCGATTTTCCATGGCAG	64.7	pJET1.2

Table 3. List of all constructs created with accompanying cDNA and plasmid backbones. Only the abbreviations are used throughout the text.

cDNA	Plasmid	Construct Name	Construct Abbreviation	Assay
UNH	pYES2/CT	pYES2/CT-UNH	UNH-pYES2/CT	yeast complementation
UNH	PBI-771	PBI771-GAL4/TA-UNH	UNH-TA	yeast two-hybrid
VPS52	PBI-771	PBI771-GAL4/TA-VPS52	VPS52-TA	yeast two-hybrid
VPS53	PBI-771	PBI771-GAL4/TA-VPS53	VPS53-TA	yeast two-hybrid
VPS54Δ552-1034 aa	PBI-771	PBI771-GAL4/TA-VPS54Δ552-1034 aa	VPS54Δ552-1034 aa-TA	yeast two-hybrid
SYP22	PBI-771	PBI771-GAL4/TA-SYP22	SYP22-TA	yeast two-hybrid
SYP41	PBI-771	PBI771-GAL4/TA-SYP41	SYP41-TA	yeast two-hybrid
SYP51	PBI-771	PBI771-GAL4/TA-SYP51	SYP51-TA	yeast two-hybrid
SYP61	PBI-771	PBI771-GAL4/TA-SYP61	SYP61-TA	yeast two-hybrid
AtRab6A	PBI-771	PBI771-GAL4/TA-AtRab6A	AtRab6A-TA	yeast two-hybrid
Vti12	PBI-771	PBI771-GAL4/TA-Vti12	Vti12-TA	yeast two-hybrid
UNHΔ1-118 aa	PBI-770	PBI771-GAL4/DB-UNHΔ1-118 aa	UNHΔ1-118 aa-DB	yeast two-hybrid
UNHΔ78-780 aa	PBI-770	PBI771-GAL4/DB-UNHΔ78-780 aa	UNHΔ78-780 aa-DB	yeast two-hybrid
UNHΔ1-289 aa	PBI-770	PBI771-GAL4/DB-UNHΔ1-289 aa	UNHΔ1-289 aa-DB	yeast two-hybrid
UNHΔ586-780 aa	PBI-770	PBI771-GAL4/DB-UNHΔ586-780 aa	UNHΔ586-780 aa-DB	yeast two-hybrid
UNH	PBI-770	PBI771-GAL4/DB-UNH	UNH-DB	yeast two-hybrid
VPS52	PBI-770	PBI771-GAL4/DB-VPS52	VPS52-DB	yeast two-hybrid
VPS53	PBI-770	PBI771-GAL4/DB-VPS53	VPS53-DB	yeast two-hybrid
VPS54Δ552-1034 aa	PBI-770	PBI771-GAL4/DB-VPS54Δ552-1034 aa	VPS54Δ552-1034 aa-DB	yeast two-hybrid
SYP61	PBI-770	PBI771-GAL4/DB-SYP61	SYP61-DB	yeast two-hybrid
UNH	pSAT1A	pSAT1A-nEYFP-UNH	UNH-nEYFP	BiFC
VPS52	pSAT4A	pSAT4A-cEYFP-VPS52	VPS52-cEYFP	BiFC
SYP61	pSAT4A	pSAT4A-cEYFP-SYP61	SYP61-cEYFP	BiFC

Figures

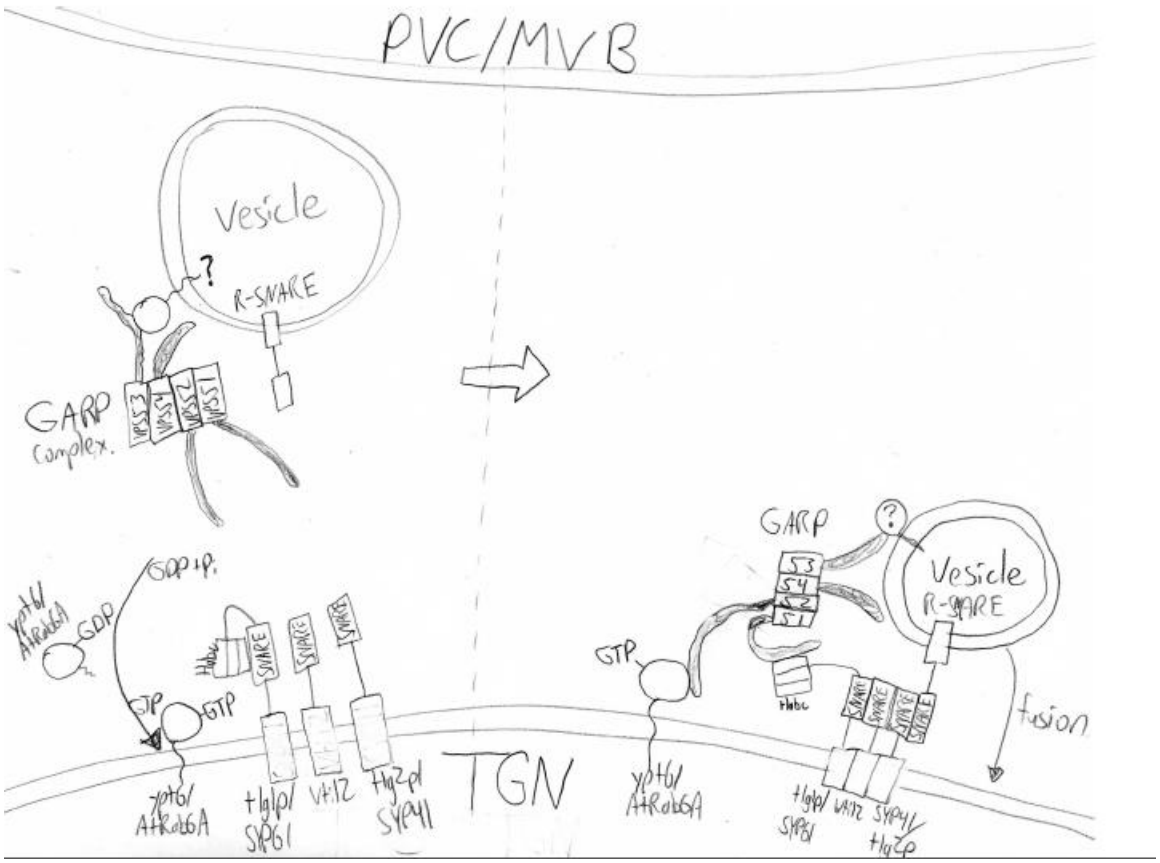

Figure 1. Diagram of proposed GARP vesicle tethering interactions during tethering of a vesicle from pre-vacuolar compartment/multi-vesicular body (PVC/MVB) with the trans-Golgi Network (TGN) in *Arabidopsis thaliana*. The diagram to the left side of the arrow depicts the proteins prior to tethering while the diagram to the right side depicts interactions occurring during tethering. The organelle membranes are indicated by the double-lines spanning the figure. Proteins are labeled with the yeast name (e.g. tlg1p, tlg2p, ypt6), followed by the putative *Arabidopsis* homologs (e,g, SYP61, SYP 41, AtRab6a). The trans-membrane domain of the SNAREs is indicated by the boxes spanning the membrane. Interactions amongst GARP N-terminal coiled coils are shown by the stacked boxes with the C-terminal regions, thought to be involved in protein interaction, indicated by the extended arms.

A)

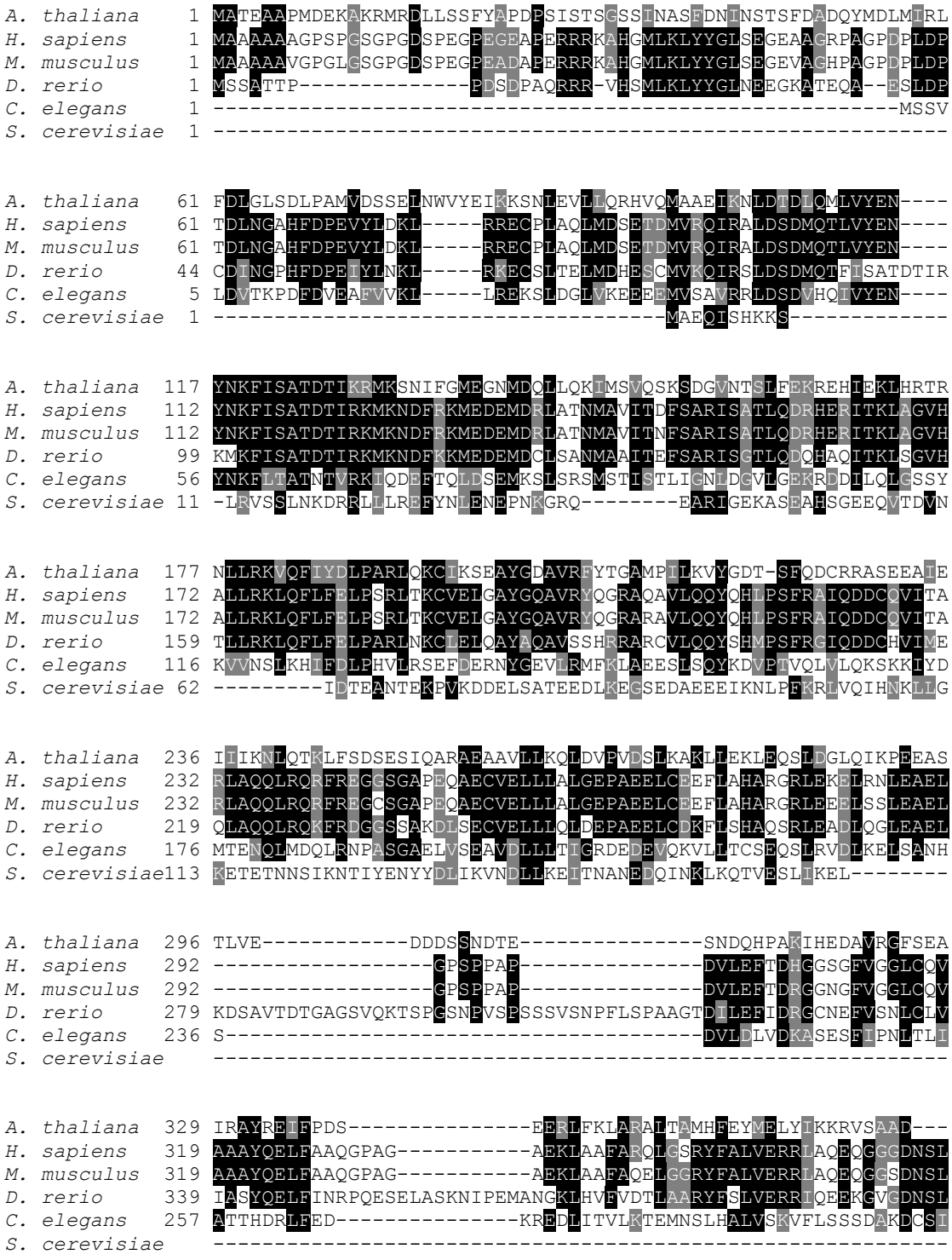
A. thaliana 1
H. sapiens 1
M. musculus 1
D. rerio 1
C. elegans 1
S. cerevisiae 1
A. thaliana 61
H. sapiens 61
M. musculus 61
D. rerio 44
C. elegans 5
S. cerevisiae 1
A. thaliana 117
H. sapiens 112
M. musculus 112
D. rerio 99
C. elegans 56
S. cerevisiae 11
A. thaliana 177
H. sapiens 172
M. musculus 172
D. rerio 159
C. elegans 116
S. cerevisiae 62
A. thaliana 236
H. sapiens 232
M. musculus 232
D. rerio 219
C. elegans 176
S. cerevisiae 113
A. thaliana 296
H. sapiens 292
M. musculus 292
D. rerio 279
C. elegans 236
S. cerevisiae
A. thaliana 329
H. sapiens 319
M. musculus 319
D. rerio 339
C. elegans 257
S. cerevisiae
A. thaliana 371
H. sapiens 368
M. musculus 368
D. rerio 399
C. elegans 302
S. cerevisiae

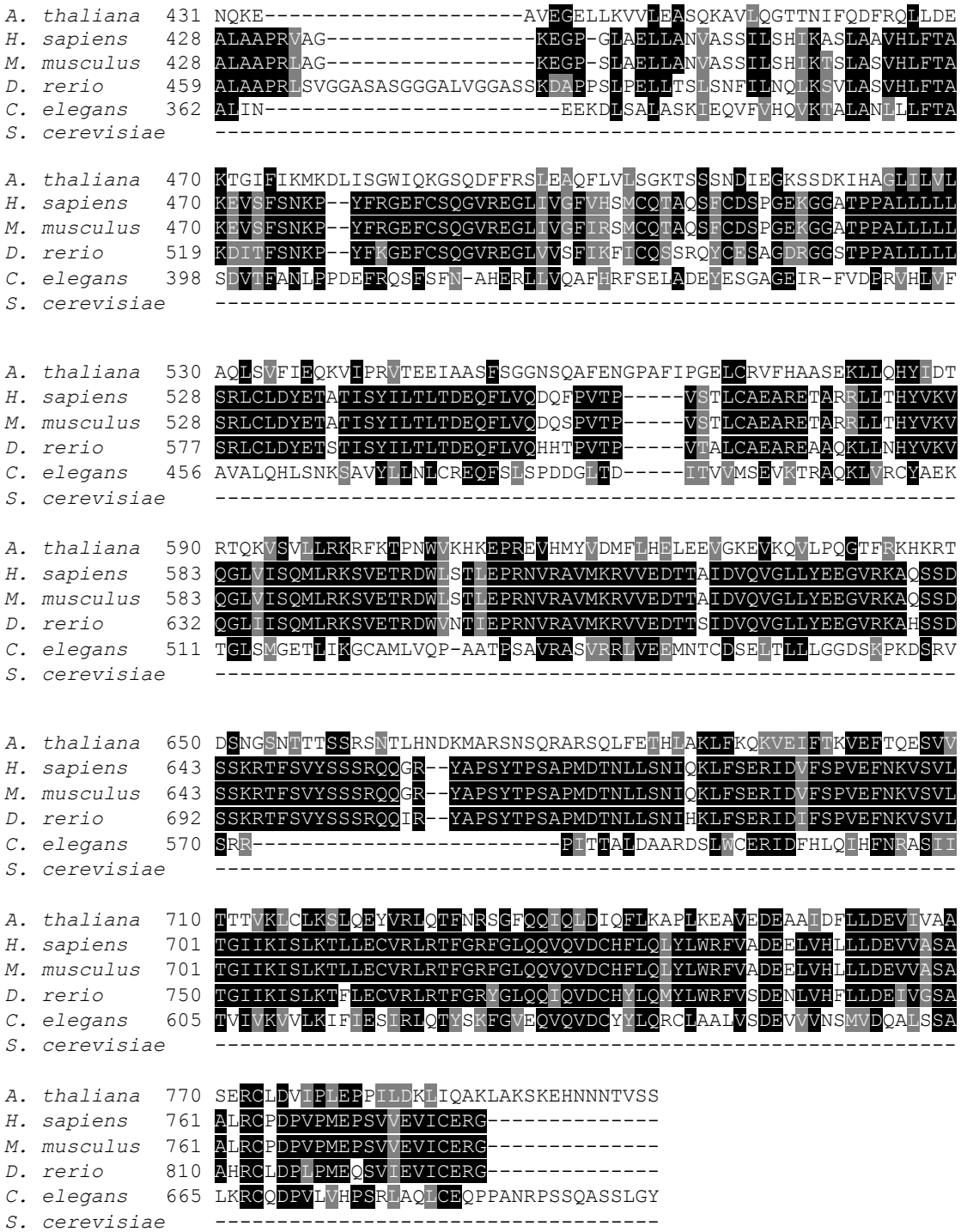
A. thaliana 431 NQKE----------AVEGELLKVVLEASQKAVLQGTTNIFQDFRQLLDE
H. sapiens 428 ALAAPRVAG----------KEGP-GLAELLANVASSILSHIKASLAAVHLFTA
M. musculus 428 ALAAPRLAG----------KEGP-SLAELLANVASSILSHIKTSLASVHLFTA
D. rerio 459 ALAAPRLSVGGASASGGGALVGGASSKDAPPSLPELLTSLSNFILNQLKSVLASVHLFTA
C. elegans 362 ALIN----------EEKDLSALASKIEQVFVHQVKTALANLLLFTA
S. cerevisiae ----------
A. thaliana 470 KTGIFIKMKDLISGWIQKGSQDFFRSLEAQFLVLSGKTSSSNDIEGKSSDKIHAGLILVL
H. sapiens 470 KEVSFSNKP--YFRGEFCSQGVREGLIVGFVHSMCQTAQSFCDSPGEKGGATPPALLLLL
M. musculus 470 KEVSFSNKP--YFRGEFCSQGVREGLIVGFIRSMCQTAQSFCDSPGEKGGATPPALLLLL
D. rerio 519 KDITFSNKP--YFKGEFCSQGVREGLVVSFIKFICQSSRQYCESAGDRGGSTPPALLLLL
C. elegans 398 SDVTFANLPPDEFRQSFSFN-AHERLLVQAFHRFSELADEYESGAGEIR-FVDPRVHLVF
S. cerevisiae ----------
A. thaliana 530 AQLSVFIEQKVIPRVTEEIAASFSGGNSQAFENGPAFIPGELCRVFHAASEKLLQHYIDT
H. sapiens 528 SRLCLDYETATISYILTLTDEQFLVQDQFPVTP-----VSTLCAEARETARRLLTHYVKV
M. musculus 528 SRLCLDYETATISYILTLTDEQFLVQDQSPVTP-----VSTLCAEARETARRLLTHYVKV
D. rerio 577 SRLCLDYETSTISYILTLTDEQFLVQHHTPVTP-----VTALCAEARETAAQKLLNHYVKV
C. elegans 456 AVALQHLSNKSAVYLLNLCREQFSLSPDDGLTD-----ITVVMSEVKTRAQKLVRCYAEK
S. cerevisiae ----------
A. thaliana 590 RTQKVSVLLRKRFKTPNWVKHKEPREVHMYVDMFLHELEEVGKEVKQVLPQGTFRKHKRT
H. sapiens 583 QGLVISQMLRKSVETRDWLSTLEPRNVRAVMKRVVEDTTAIDVQVGLLYEEGVRKAQSSD
M. musculus 583 QGLVISQMLRKSVETRDWLSTLEPRNVRAVMKRVVEDTTAIDVQVGLLYEEGVRKAQSSD
D. rerio 632 QGLIISQMLRKSVETRDWVNTIEPRNVRAVMKRVVEDTTSIDVQVGLLYEEGVRKAHSSD
C. elegans 511 TGLSMGETLIKGCAMLVQP-AATPSAVRASVRRLVEEMNTCDSELTLLLGGDSKPKDSRV
S. cerevisiae ----------
A. thaliana 650 DSNGSNTTTSSRSNTLHNDKMARSNSQRARSQLFETHLAKLFKQKVEIFTKVEFTQESVV
H. sapiens 643 SSKRTFSVYSSSRQQGR--YAPSYTPSAPMDTNLLSNIQKLFSERIDVFSPVEFNKVSVL
M. musculus 643 SSKRTFSVYSSSRQQGR--YAPSYTPSAPMDTNLLSNIQKLFSERIDVFSPVEFNKVSVL
D. rerio 692 SSKRTFSVYSSSRQQIR--YAPSYTPSAPMDTNLLSNIHKLFSERIDIFSPVEFNKVSVL
C. elegans 570 SRR----------PITTALDAARDSLWCERIDFHLQIHFNRASII
S. cerevisiae ----------
A. thaliana 710 TTTVKLCLKSLQEYVRLQTFNRSGFQQIQLDIQFLKAPLKEAVEDEAAIDFLLDEVIVAA
H. sapiens 701 TGIIKISLKTLLECVRLRTFGRFGLQQVQVDCHFLQLYLWRFVADEELVHLLLDEVVASA
M. musculus 701 TGIIKISLKTLLECVRLRTFGRFGLQQVQVDCHFLQLYLWRFVADEELVHLLLDEVVASA
D. rerio 750 TGIIKISLKTFLECVRLRTFGRYGLQQIQVDCHYLQMYLWRFVSDENLVHFLLDEIVGSA
C. elegans 605 TVIVKVVLKIFIESIRLQTYSKFGVEQVQVDCYYLQRCLAALVSDEVVVNSMVDQALSSA
S. cerevisiae ----------
A. thaliana 770 SERCLDVIPLEPPILDKLIQAKLAKSKEHNNNTVSS
H. sapiens 761 ALRCPDPVPMEPSVVEVICERG----------
M. musculus 761 ALRCPDPVPMEPSVVEVICERG----------
D. rerio 810 AHRCLDPLPMEQSVIEVICERG----------
C. elegans 665 LKRCQDPVLVHPSRLAQLCEQPPANRPSSQASSLGY
S. cerevisiae ----------

B)

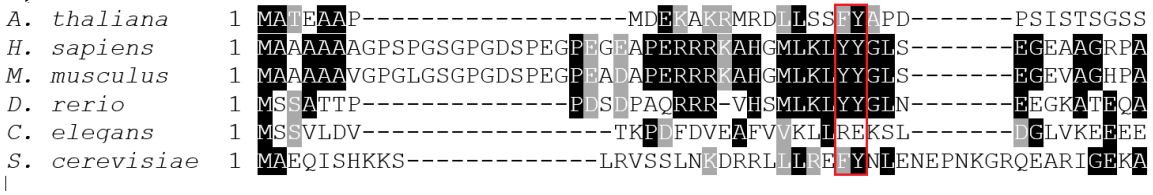

C)

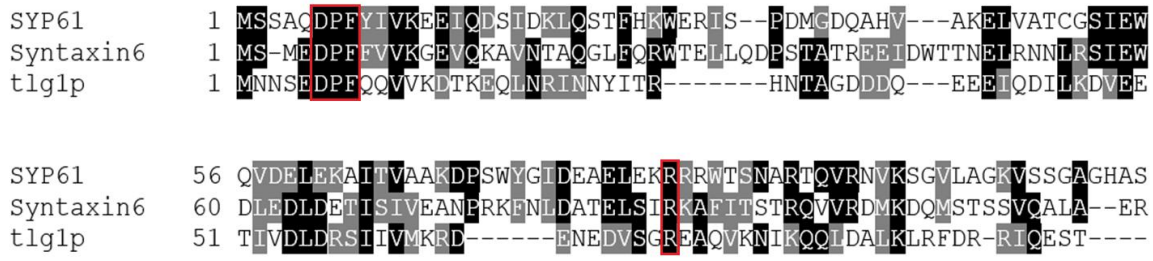

Figure 2. A) Multiple sequence alignment of VPS51 orthologues from representative eukaryotes. Entire protein length was used in the alignment. B) Sequence comparison of the N-terminal region containing the di-tyrosine motif (only N-terminal sequence used in alignment, motif highlighted in red) C) Sequence comparison of N-terminal H_{abc} domain of SYP61 orthologues (motif highlighted in red). Amino acid numbers for start of respective sequence displayed on the left. CLUSTAL W and BOXSHADE were used to perform alignment and shading of amino acids respectively. Identical and conserved amino acids highlighted in black and grey respectively. Amino acid sequence data used for alignment can be found in UniProt under the following accession numbers: *Arabidopsis thaliana* UNHINGED/VPS51 (UniProtKB: F4JH69), *M. musculus* VPS51 (UniProtKB: Q3UVL4), *H. sapiens* Ang2/VPS51 (UniProtKB: Q9UID3), *D. rerio* VPS51/ffr (UniProtKB: Q155U0), *S. cerevisiae* VPS51/YKR020W (UniProtKB: P36116), *C. elegans* VPS51/B0414.8b (UniProtKB: G8XYY4), *A. thaliana* SYP61 (UniProtKB: Q946Y7), *H. sapiens* SYX6 (UniProtKB: O43752), *S. cerevisiae* tlg1p (UniProtKB: E7Q2Q7).

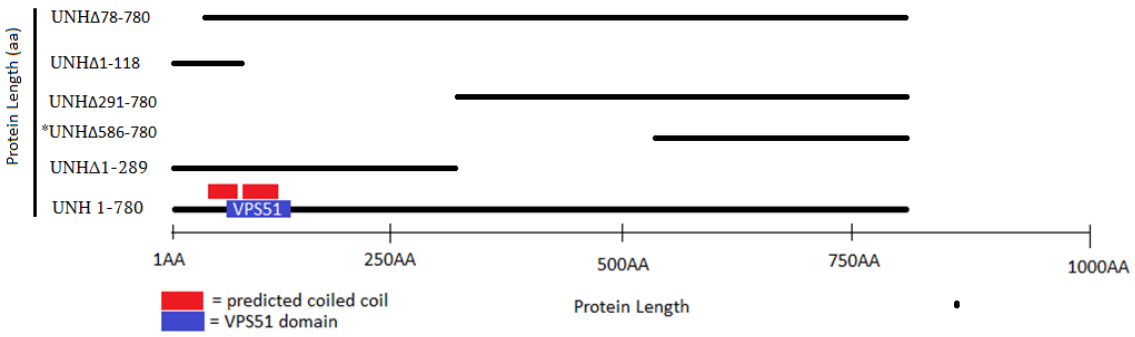

UNHINGED truncated mutant	Forward Primer	Reverse Primer
UNHΔ78-780	Primer_ATW_leftborder_NewRev2	Primer_ATW_leftborder_Fwd1
UNHΔ1-118	Primer_ATW_rightborder_Fwd	Primer_ATW_rightborder_rev5
UNHΔ291-780	Primer_ATW_leftborder_NewRev2	Primer_ATW_leftborder_Fwd3
*UNHΔ586-780	Primer_ATW_leftborder_NewRev2	Primer_ATW_leftborder_Fwd3
UNHΔ1-289	Primer_ATW_rightborder_Fwd	Primer_ATW_rightborder_rev6

Figure 3. Diagram of truncated UNHINGED mutant sizes above full length protein (1-780 aa). Truncated versions were generated using around-the-world PCR primers listed in table. * Primer incorrectly bound to region of UNHINGED resulting in a smaller C-terminal fragment.

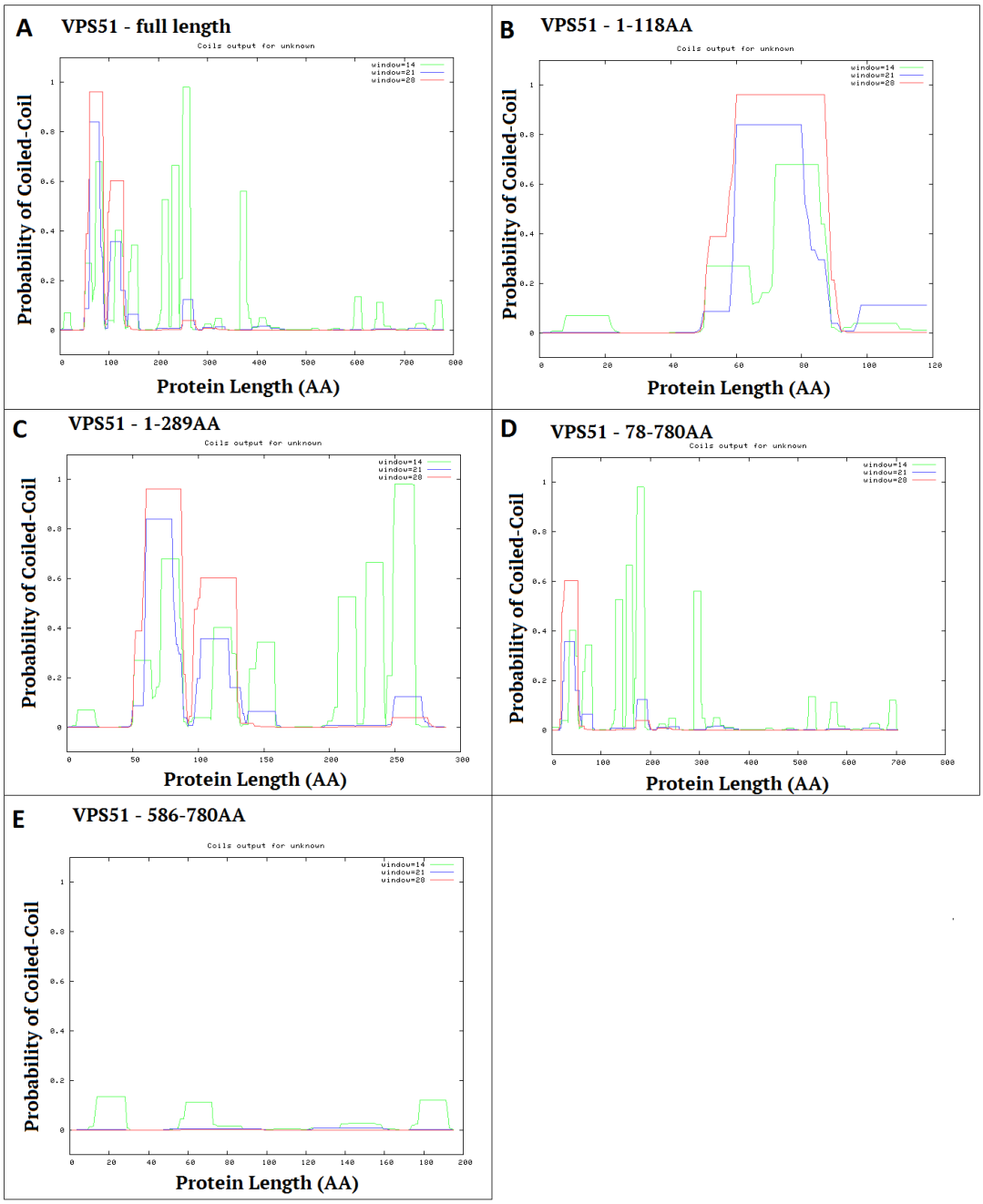

Figure 4. Predicted coiled-coil domains of full *Arabidopsis thaliana* VPS51 and truncated mutants. Probability of coiled-coil domains for the amino acid window length 14, 21 and 28 are displayed in green, blue and red, respectively (N-terminal = amino acid position 1). COILS server used to predict coils via http://www.ch.embnet.org/software/COILS_form.html.

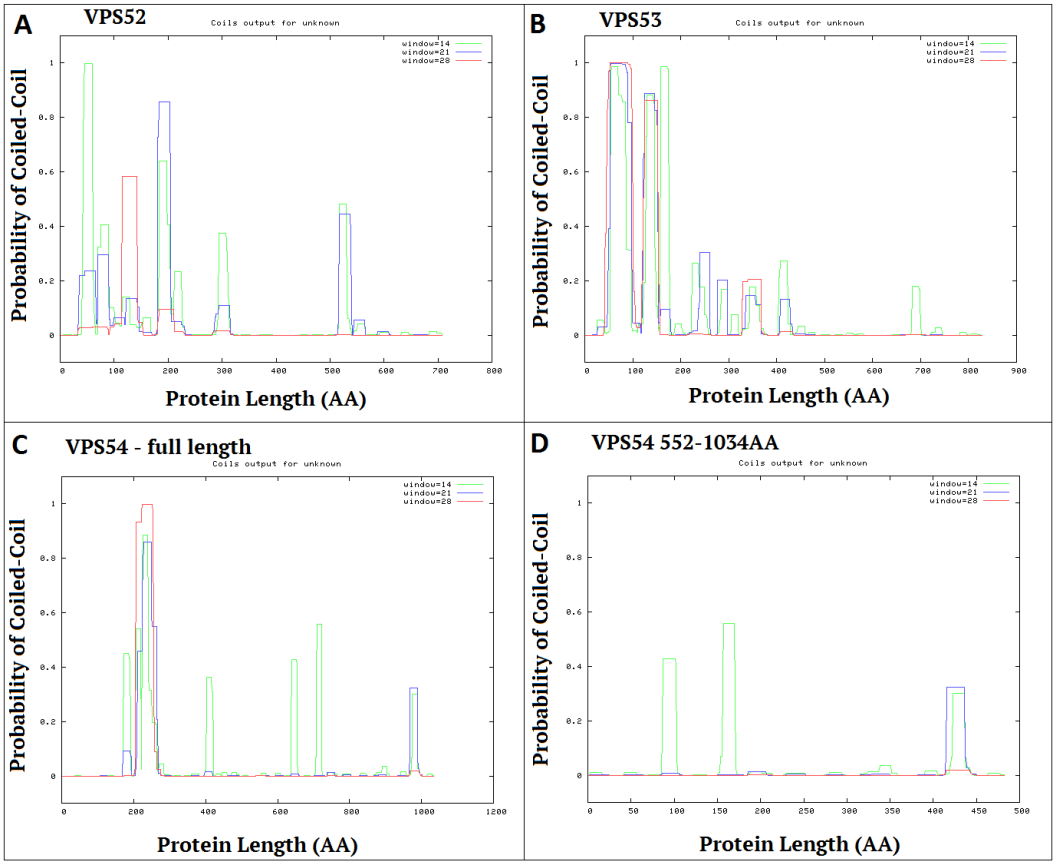

Figure 5. Predicted coiled-coil domains of *Arabidopsis thaliana* VPS52, VPS53 and both C-terminal and full length VPS54 subunits. Probability of coiled-coil domains for the amino acid window length 14, 21 and 28 are displayed in green, blue and red, respectively (N-terminal = amino acid position 1). COILS server used to predict coils via http://www.ch.embnet.org/software/COILS_form.html.

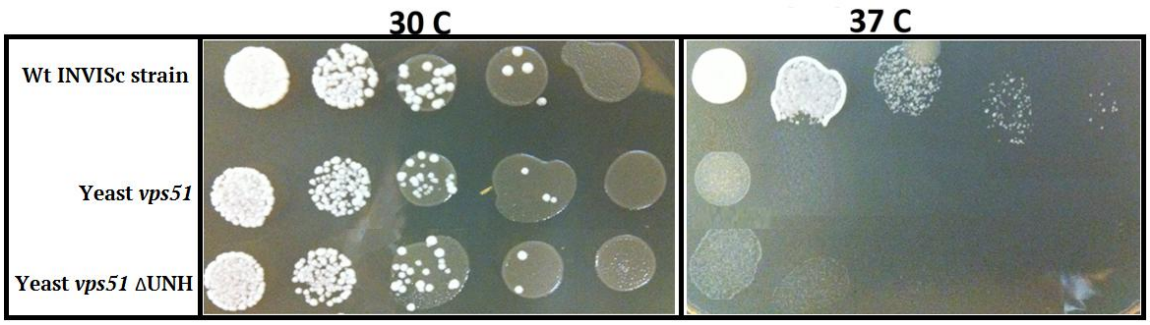

Figure 6. Yeast complementation assay comparing growth properties of wildtype (INVISc), *vps51*, and *vps51* **Δ**UNHINGED. Yeast *vps51* **Δ**UNHINGED was transformed with UNHINGED in the pYES2/CT vector. Sequentially diluted yeast was spotted on YEPD media plates at 30°C and 37°C for 2 days.

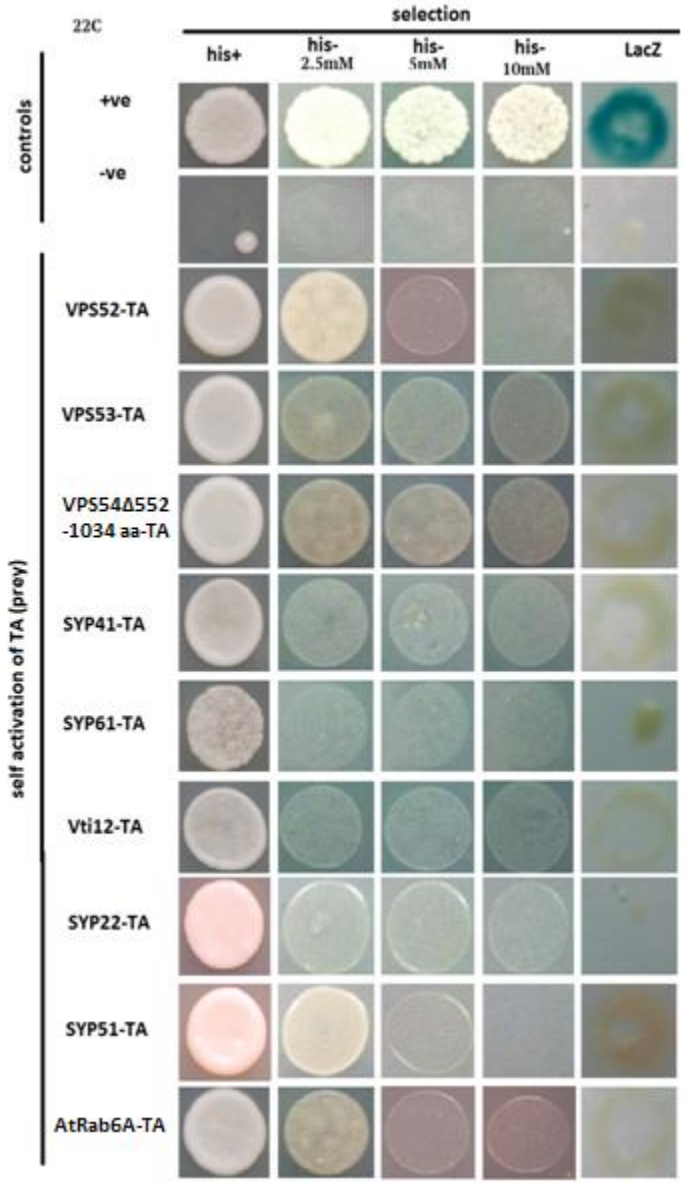

Figure 7. Yeast two-hybrid testing the self-activation of proteins fused to the Gal4 activating domain of pbi-771. Yeast are transformed with individual vectors of various protein coding regions fused to the GAL4 activating domain (labeled on left side). First row contains positive control (AGL4-T4 + empty TA) and second row shows negative control (AGL4-T7 + empty DB). Column 1: media containing histidine and acted as the growth control. Columns 2-4: assessed HIS3 expression on media lacking histidine and supplemented with 2.5 mM, 5 mM and 10 mM 3-AT. Column 5: assessed expression of LacZ by exposing yeast for 4 hours in Z-buffer with X-gal (LacZ cleaves X-gal, making a blue color). All yeast was grown at 22°C for 4 days before being tested.

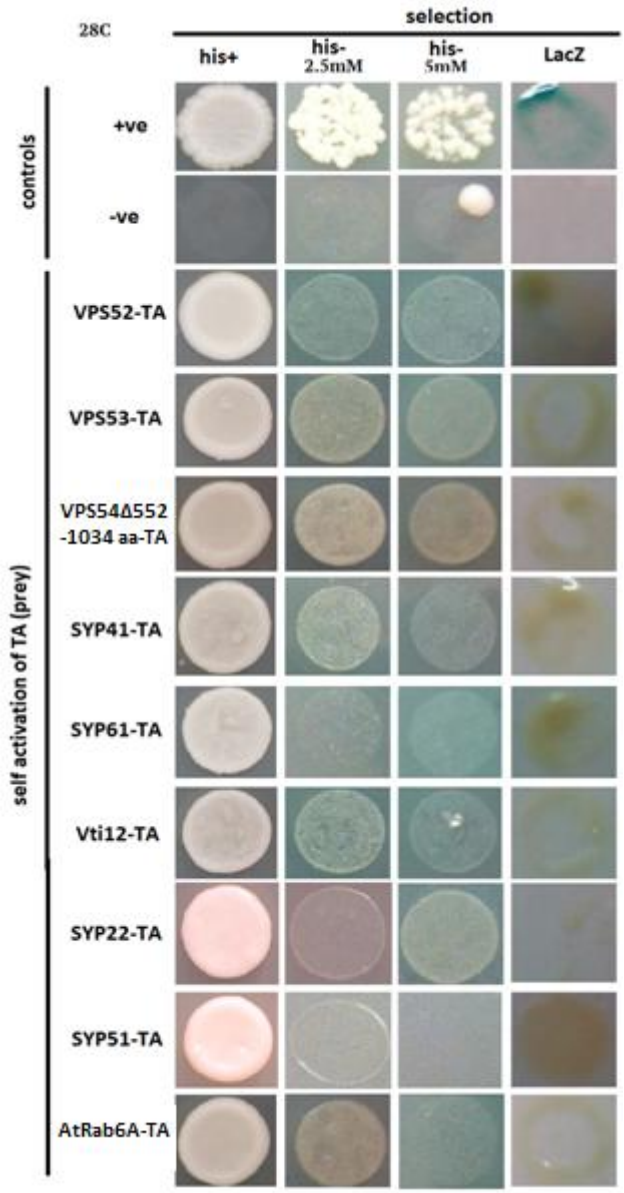

Figure 8. Yeast two-hybrid testing the self-activation of proteins fused to the Gal4 activating domain of pbi-771. Yeast are transformed with individual vectors of various protein coding regions fused to the GAL4 activating domain (labeled on left side). First row contains positive control (AGL4-T4 + empty TA) and second row shows negative control (AGL4-T7 + empty DB). Column 1: media containing histidine and acted as the growth control. Columns 2-3: assessed HIS3 expression on media lacking histidine and supplemented with 2.5 mM and 5 mM. Column 4: assessed expression of LacZ by exposing yeast for 4 hours in Z-buffer with X-gal (LacZ cleaves X-gal, making a blue color). All yeast was grown at 28°C for 4 days before being tested.

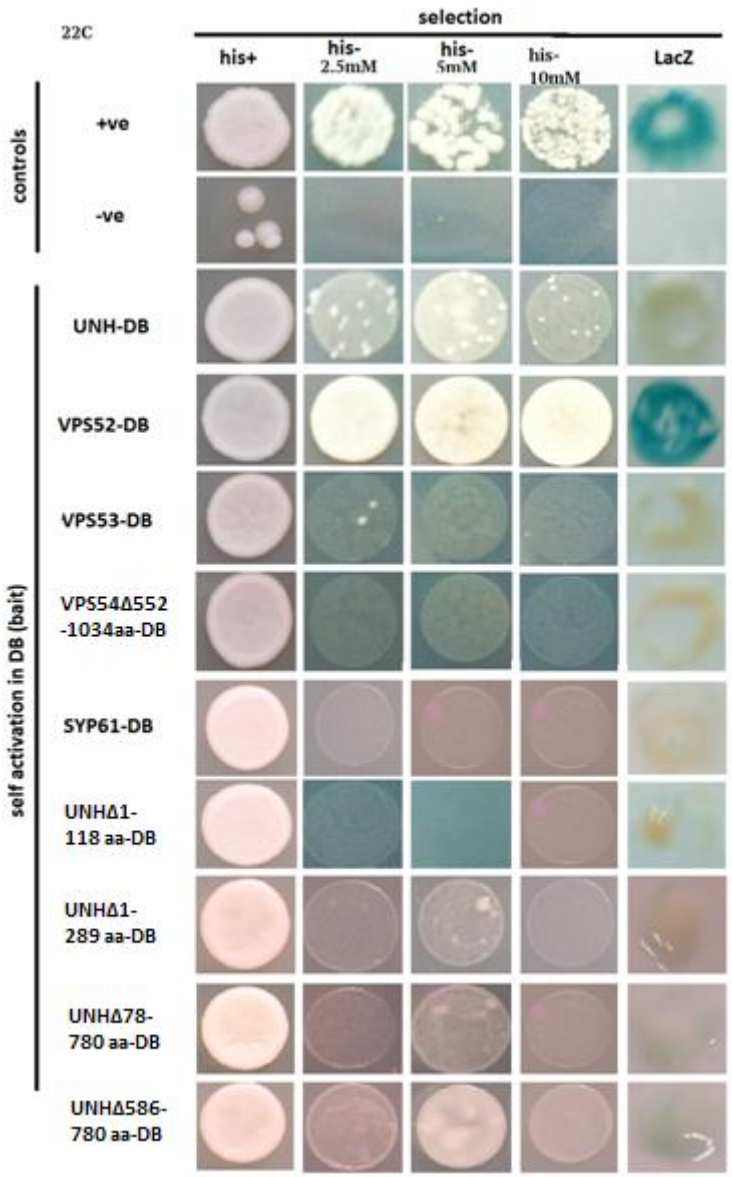

Figure 9. Yeast two-hybrid testing the self-activation of proteins fused to the Gal4 DB domain of pbi-770. Yeast are transformed with individual vectors of various protein coding regions fused to the GAL4 activating domain (labeled on left side). First row contains positive control (AGL4-T4 + empty TA) and second row shows negative control (AGL4-T7 + empty DB). Column 1: media containing histidine and acted as the growth control. Columns 2-4: assessed HIS3 expression on media lacking histidine and supplemented with 2.5 mM, 5 mM and 10 mM 3-AT. Column 5: assessed expression of LacZ by exposing yeast for 4 hours in Z-buffer with X-gal (LacZ cleaves X-gal, making a blue color). All yeast was grown at 22°C for 4 days before being tested.

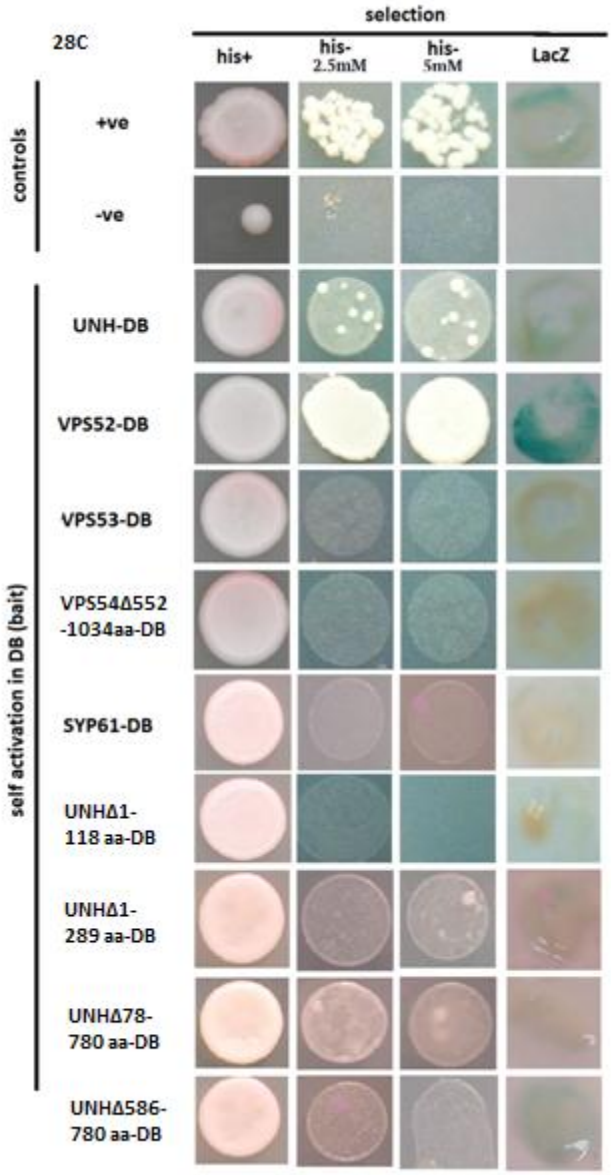

Figure 10. Yeast two-hybrid testing the self-activation of proteins fused to the Gal4 DB domain of pbi-770. Yeast are transformed with individual vectors of various protein coding regions fused to the GAL4 activating domain (labeled on left side). First row contains positive control (AGL4-T4 + empty TA) and second row shows negative control (AGL4-T7 + empty DB). Column 1: media containing histidine and acted as the growth control. Columns 2-3: assessed HIS3 expression on media lacking histidine and supplemented with 2.5 mM and 5 mM 3-AT. Column 5: assessed expression of LacZ by exposing yeast for 4 hours in Z-buffer with X-gal (LacZ cleaves X-gal, making a blue color). All yeast was grown at 28°C for 4 days before being tested.

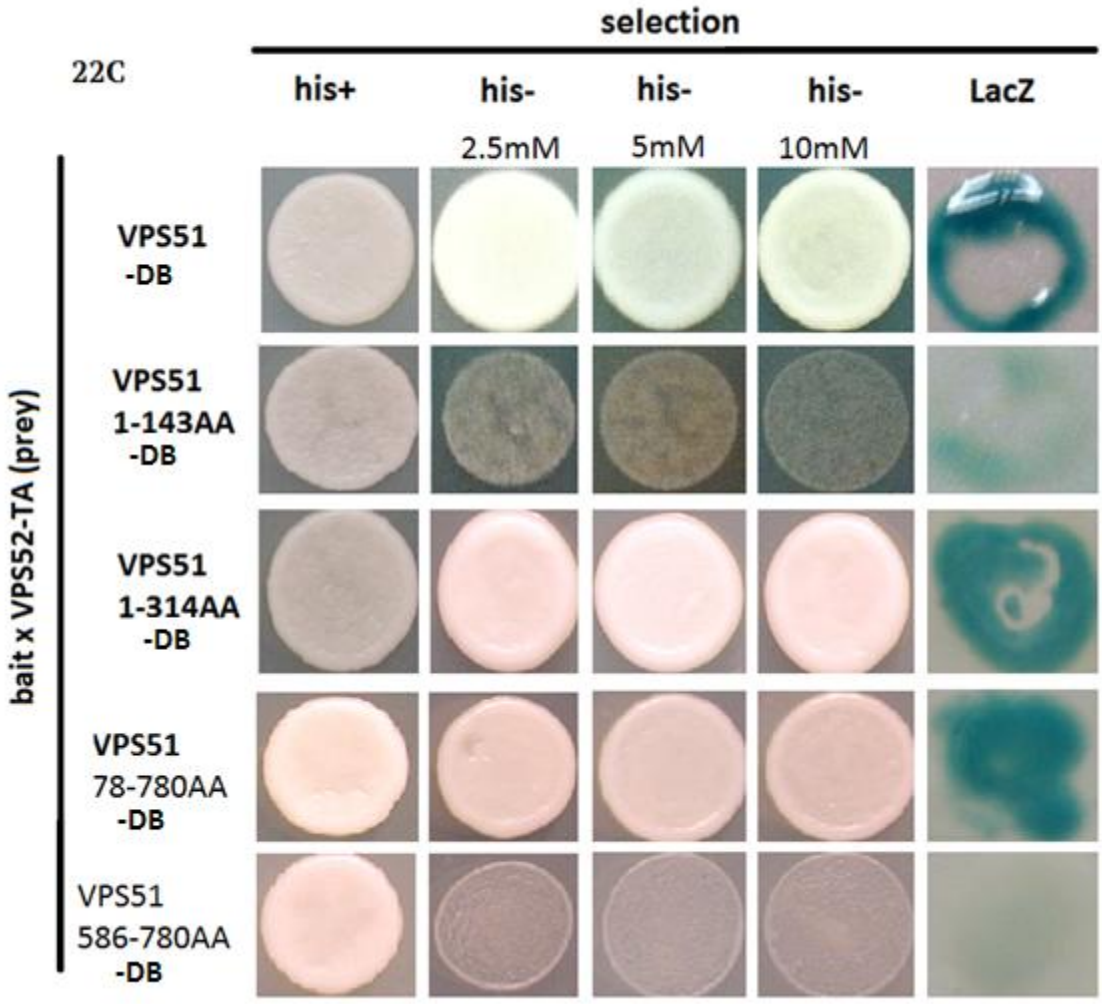

Figure 11. Yeast two-hybrid testing interactions between UNHINGED truncated mutants fused to the GAL4-DB with VPS52 fused to the GAL4 TA domain of pbi-771. Column 1: media containing histidine and acted as the growth control. Columns 2-4: assessed HIS3 expression on media lacking histidine and supplemented with 2.5 mM, 5 mM and 10 mM 3-AT. Column 5: assessed expression of LacZ by exposing yeast for 4 hours in Z-buffer with X-gal (LacZ cleaves X-gal, making a blue color). All yeast was grown at 22°C for 4 days before being tested.

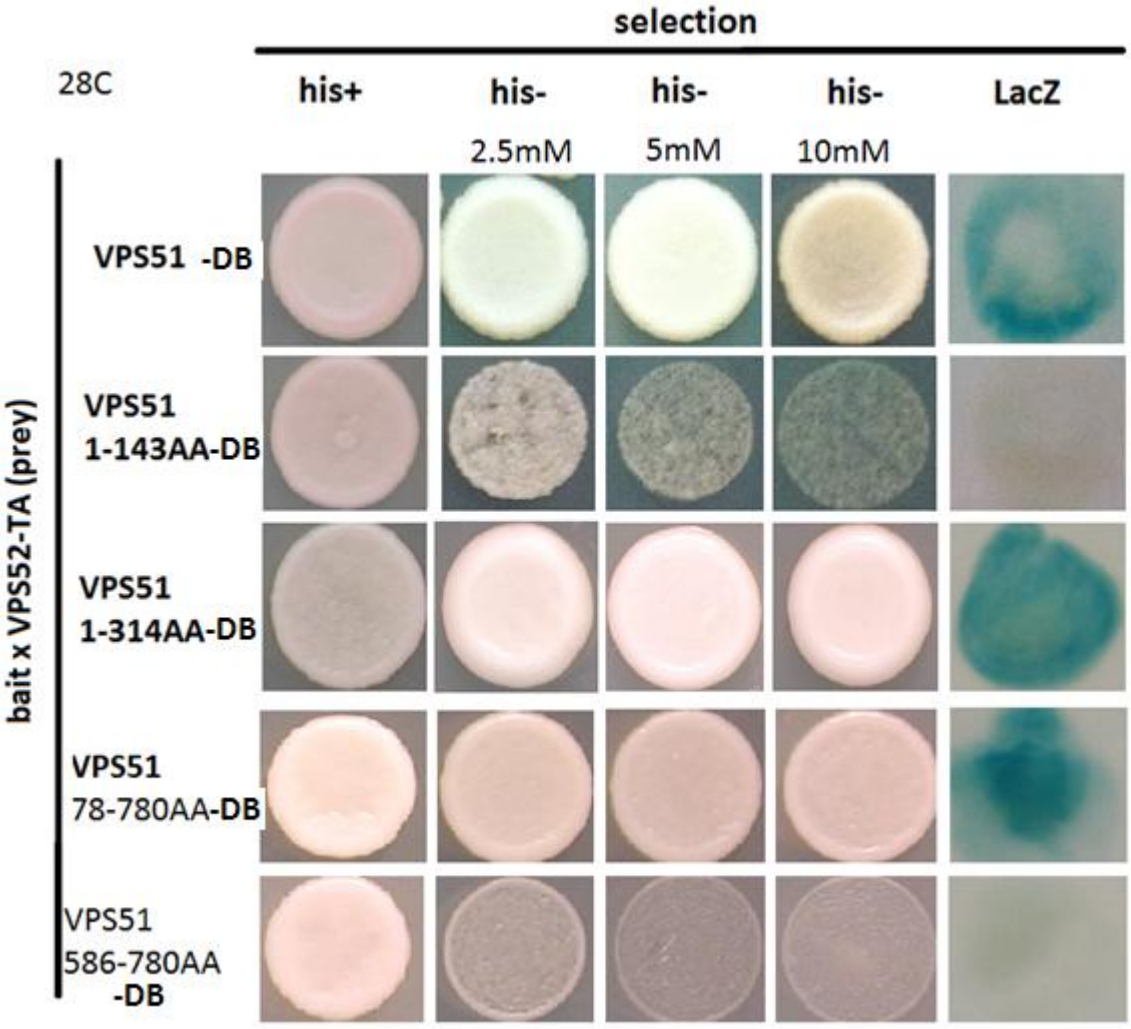

Figure 12. Yeast two-hybrid testing interactions between UNHINGED truncated mutants fused to the GAL4-DB with VPS52 fused to the GAL4 TA domain of pbi-771. Column 1: media containing histidine and acted as the growth control. Columns 2-4: assessed HIS3 expression on media lacking histidine and supplemented with 2.5 mM, 5 mM and 10 mM 3-AT. Column 5: assessed expression of LacZ by exposing yeast for 4 hours in Z-buffer with X-gal (LacZ cleaves X-gal, making a blue color). All yeast was grown at 28°C for 4 days before being tested.

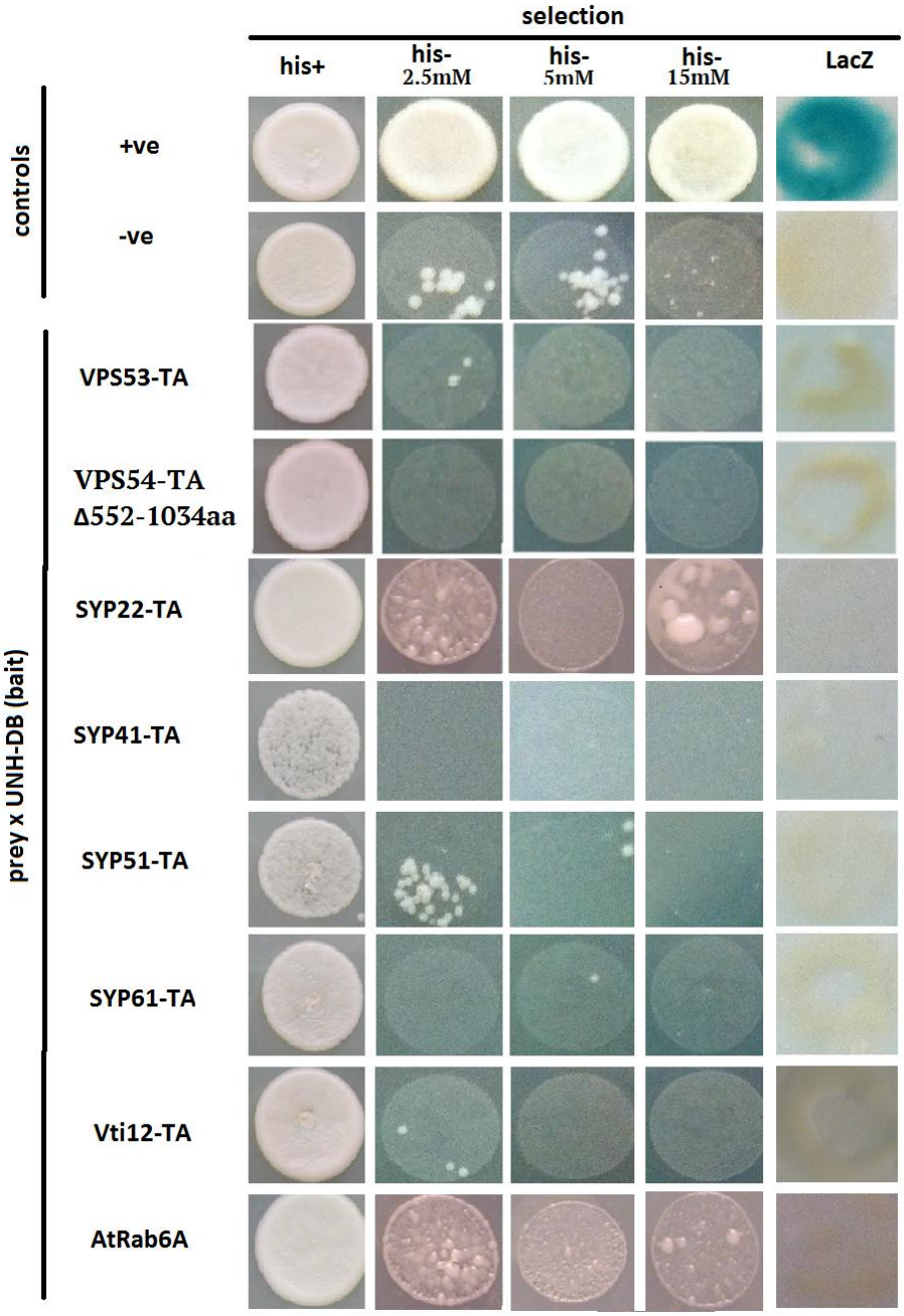

Figure 13. Yeast two-hybrid testing interactions between UNHINGED fused to the GAL4-DB of pbi-770 with various SNAREs and AtRab6A fused to the GAL4 TA domain of pbi-771. First row contains positive control (AGL4-T4 + empty TA) and second row shows negative control (AGL4-T7 + empty DB). Column 1: media containing histidine and acted as the growth control. Columns 2-4: assessed HIS3 expression on media lacking histidine and supplemented with 2.5 mM, 5 mM and 10 mM 3-AT. Column 5: assessed expression of LacZ by exposing yeast for 4 hours in Z-buffer with X-gal (LacZ cleaves X-gal, making a blue color). All yeast was grown at 22°C for 4 days before being tested.

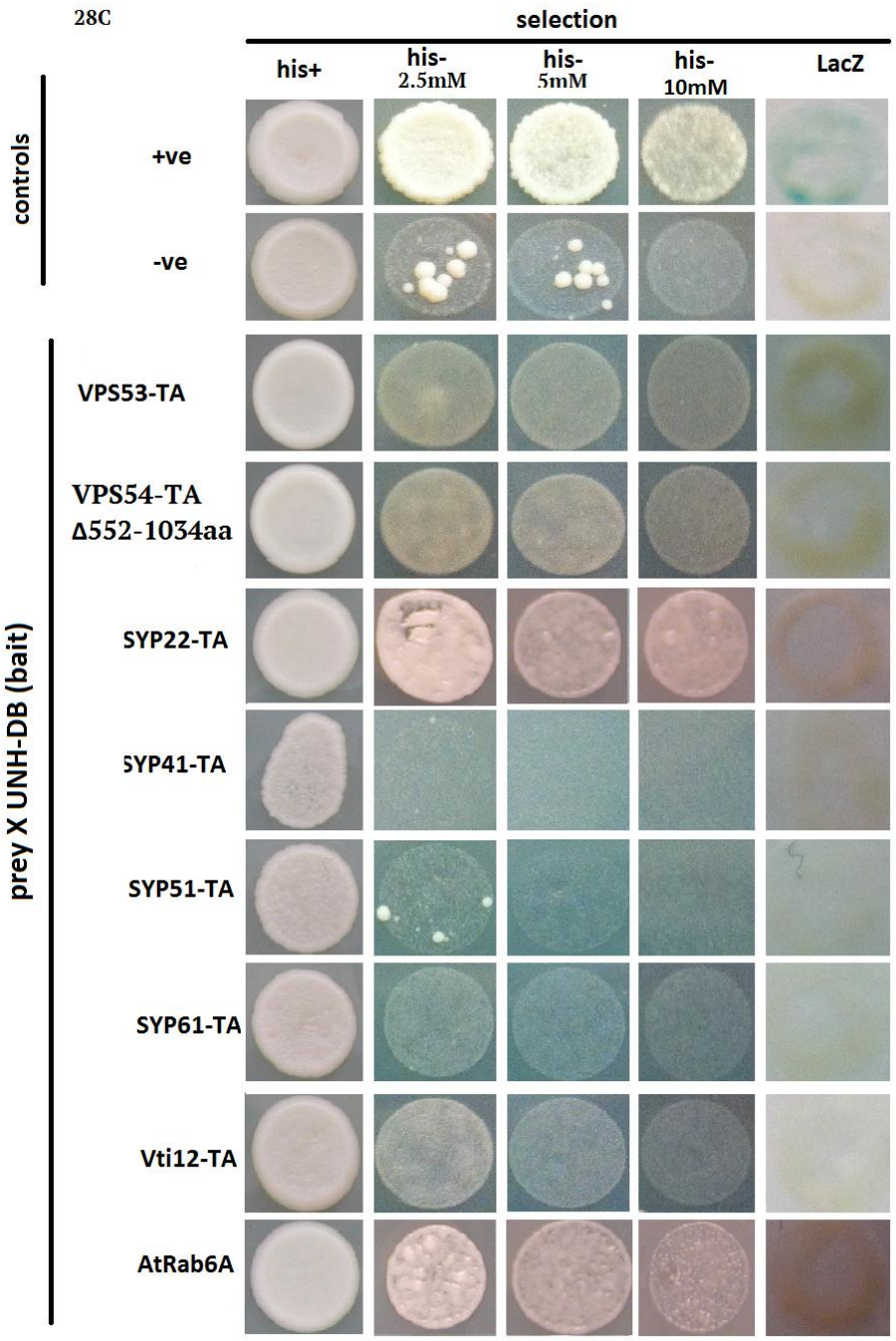

Figure 14. Yeast two-hybrid testing interactions between UNHINGED fused to the GAL4-DB with various SNAREs and AtRab6A fused to the GAL4 TA domain of pbi-771. First row contains positive control (AGL4-T4 + empty TA) and second row shows negative control (AGL4-T7 + empty DB). Column 1: media containing histidine and acted as the growth control. Columns 2-4: assessed HIS3 expression on media lacking histidine and supplemented with 2.5 mM, 5 mM and 10 mM 3-AT. Column 5: assessed expression of LacZ by exposing yeast for 4 hours in Z-buffer with X-gal (cleaves X-gal, making a blue color). All yeast was grown at 28°C for 4 days.

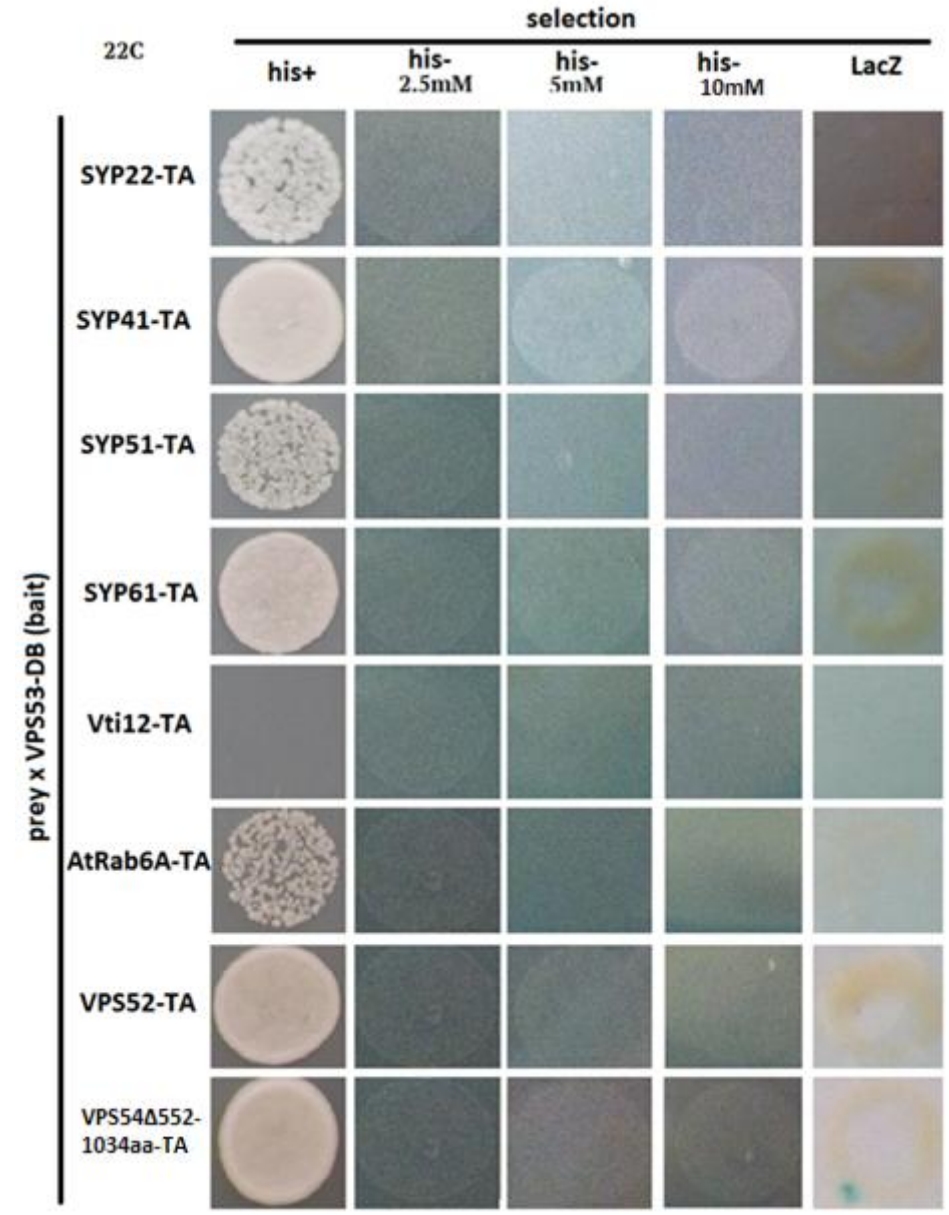

Figure 15. Yeast two-hybrid testing interactions between VPS53 fused to the GAL4-DB with various SNAREs and AtRab6A fused to the GAL4 TA domain of pbi-771. Column 1: media containing histidine and acted as the growth control. Columns 2-4: assessed HIS3 expression on media lacking histidine and supplemented with 2.5 mM, 5 mM and 10 mM 3-AT. Column 5: assessed expression of LacZ by exposing yeast for 4 hours in Z-buffer with X-gal (cleaves X-gal, making a blue color). All yeast was grown at 22°C for 4 days prior to testing.

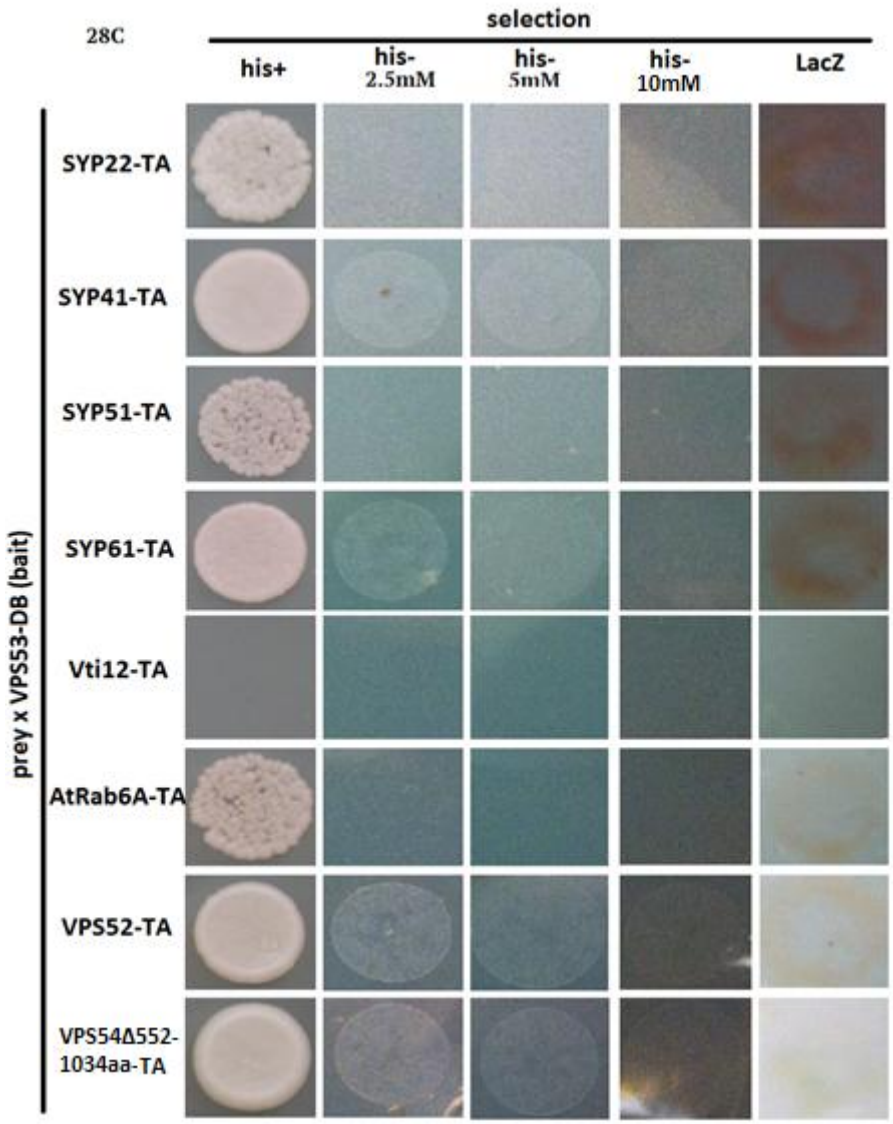

Figure 16. Yeast two-hybrid testing interactions between VPS53 fused to the GAL4-DB with various SNAREs and AtRab6A fused to the GAL4 TA domain of pbi-771. Column 1: media containing histidine and acted as the growth control. Columns 2-4: assessed HIS3 expression on media lacking histidine and supplemented with 2.5 mM, 5 mM and 10 mM 3-AT. Column 5: assessed expression of LacZ by exposing yeast for 4 hours in Z-buffer with X-gal (cleaves X-gal, making a blue color). All yeast was grown at 28°C for 4 days prior to testing.

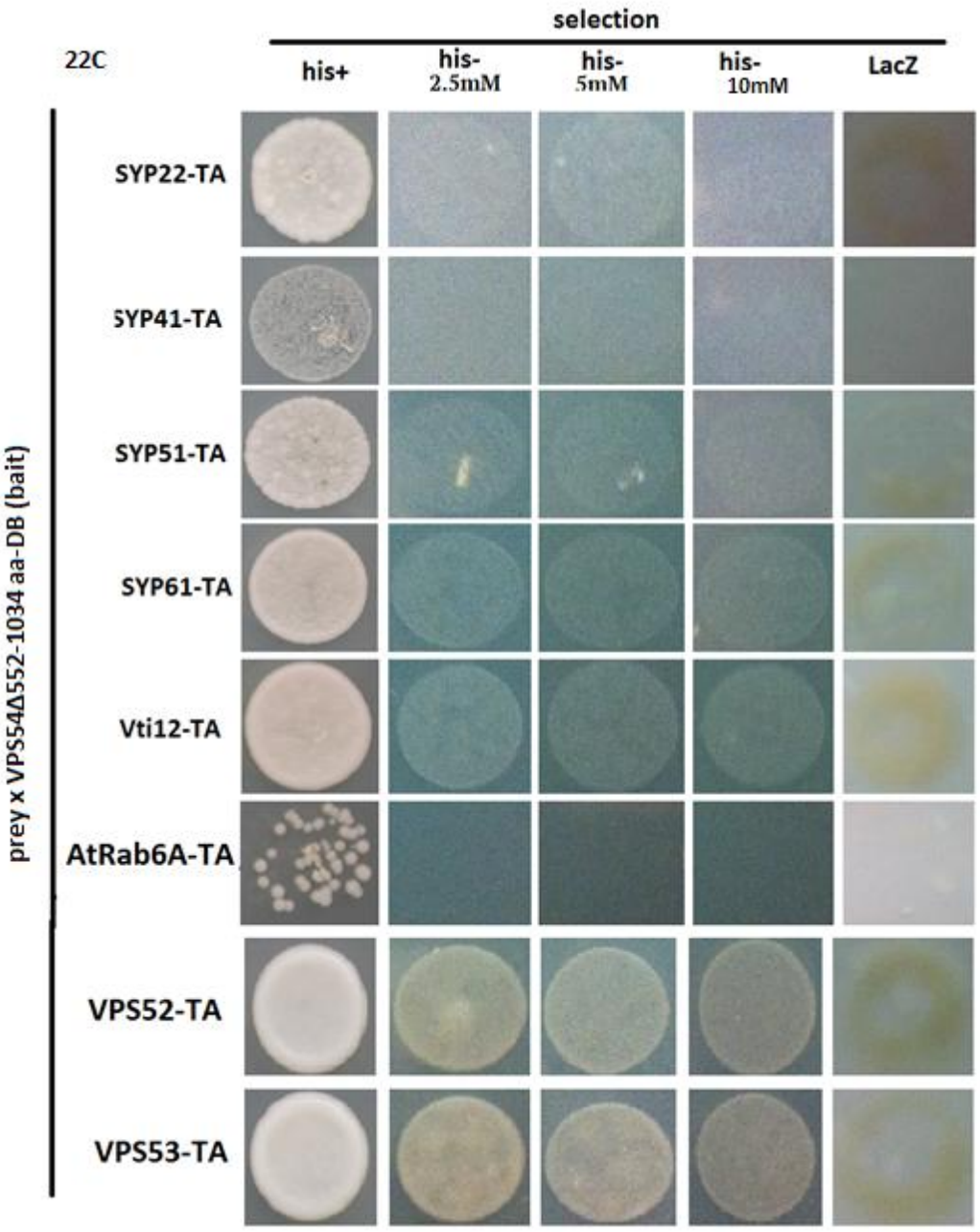

Figure 17. Yeast two-hybrid testing interactions between VPS54 fused to the GAL4-DB with various SNAREs and AtRab6A fused to the GAL4 TA domain of pbi-771. Column 1: media containing histidine and acted as the growth control. Columns 2-4: assessed HIS3 expression on media lacking histidine and supplemented with 2.5 mM, 5 mM and 10 mM 3-AT. Column 5: assessed expression of LacZ by exposing yeast for 4 hours in Z-buffer with X-gal (cleaves X-gal, making a blue color). All yeast was grown at 22°C for 4 days prior to testing.

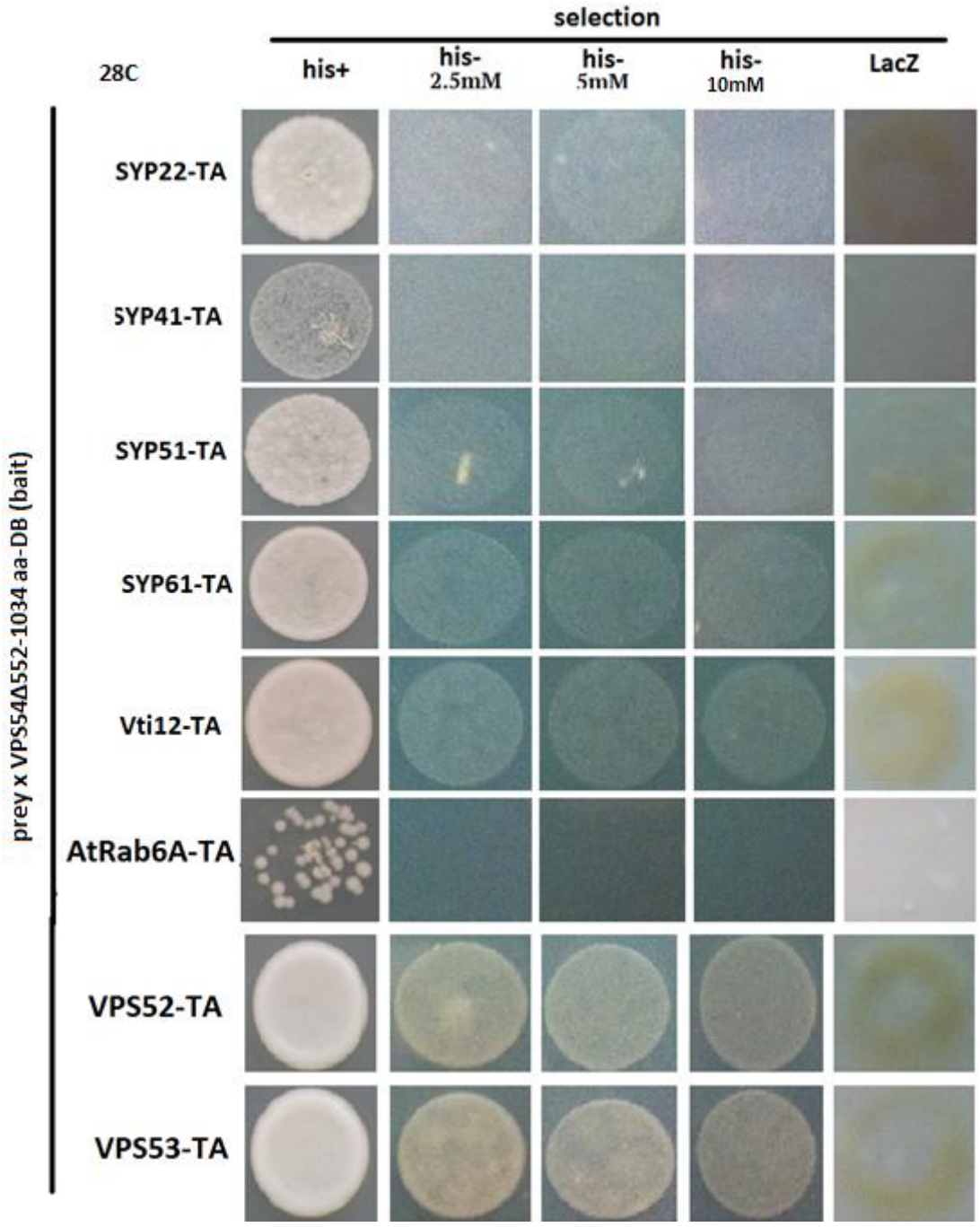

Figure 18. Yeast two-hybrid testing interactions between VPS54 fused to the GAL4-DB with various SNAREs and AtRab6A fused to the GAL4 TA domain of pbi-771. Column 1: media containing histidine and acted as the growth control. Columns 2-4: assessed HIS3 expression on media lacking histidine and supplemented with 2.5 mM, 5 mM and 10 mM 3-AT. Column 5: assessed expression of LacZ by exposing yeast for 4 hours in Z-buffer with X-gal (cleaves X-gal, making a blue color). All yeast was grown at 28°C for 4 days prior to testing.

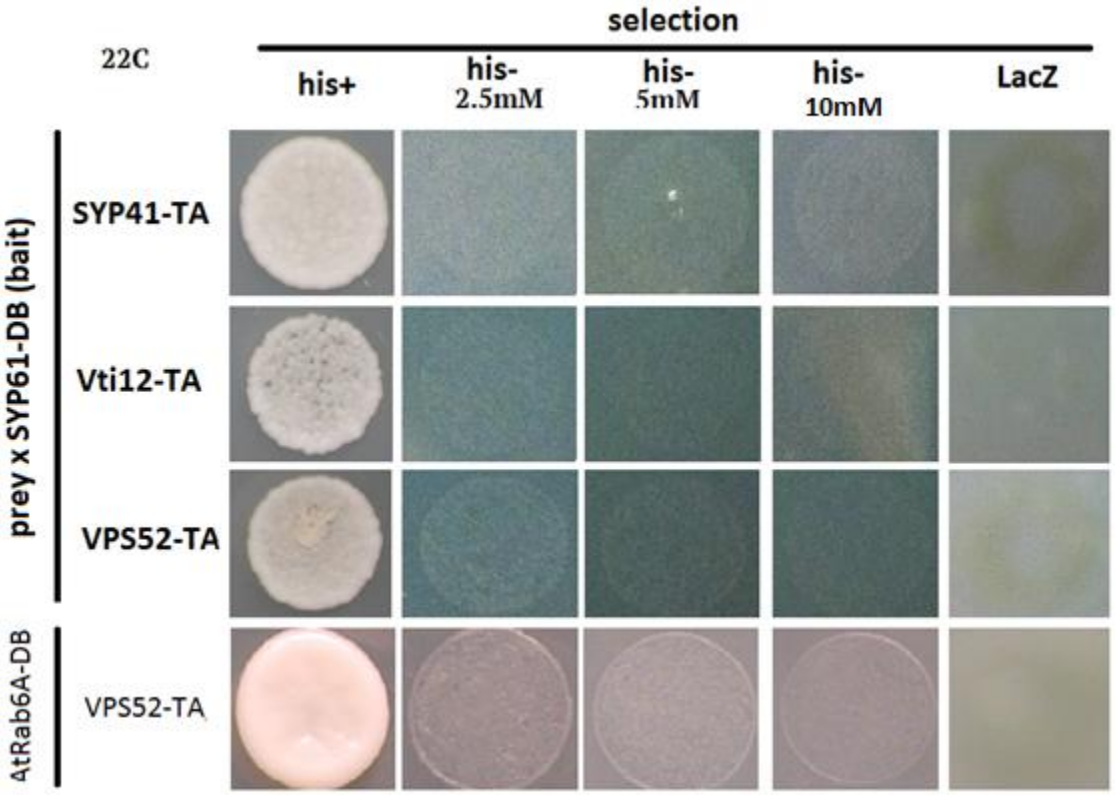

Figure 19. Yeast two-hybrid testing interactions between either SYP61 or VPS52 fused to the GAL4-DB with vti12, SYP41 and VPS52 fused to the GAL4 TA domain of pbi-771. Column 1: media containing histidine and acted as the growth control. Columns 2-4: assessed HIS3 expression on media lacking histidine and supplemented with 2.5 mM, 5 mM and 10 mM 3-AT. Column 5: assessed expression of LacZ by exposing yeast for 4 hours in Z-buffer with X-gal (cleaves X-gal, making a blue color). All yeast was grown at 22°C for 4 days prior to testing.

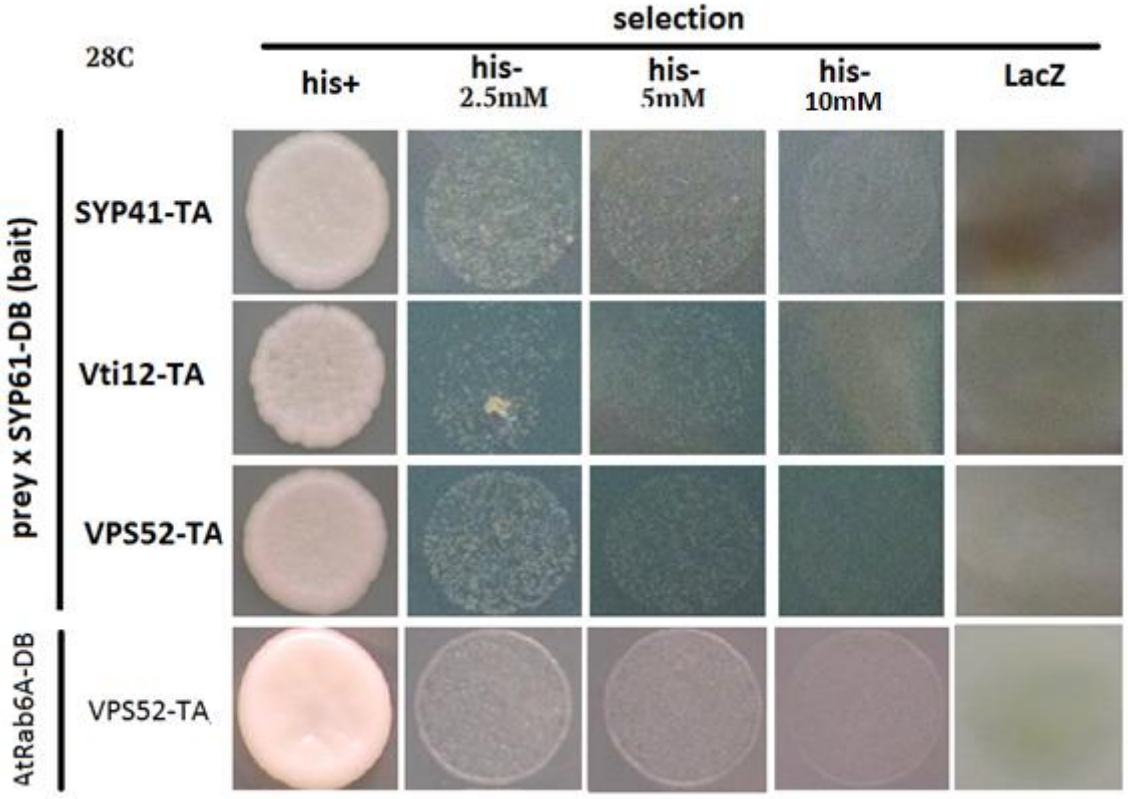

Figure 20. Yeast two-hybrid testing interactions between either SYP61 or VPS52 fused to the GAL4-DB with vti12, SYP41 and VPS52 fused to the GAL4 TA domain of pbi-771. Column 1: media containing histidine and acted as the growth control. Columns 2-4: assessed HIS3 expression on media lacking histidine and supplemented with 2.5 mM, 5 mM and 10 mM 3-AT. Column 5: assessed expression of LacZ by exposing yeast for 4 hours in Z-buffer with X-gal (cleaves X-gal, making a blue color). All yeast was grown at 28°C for 4 days prior to testing.

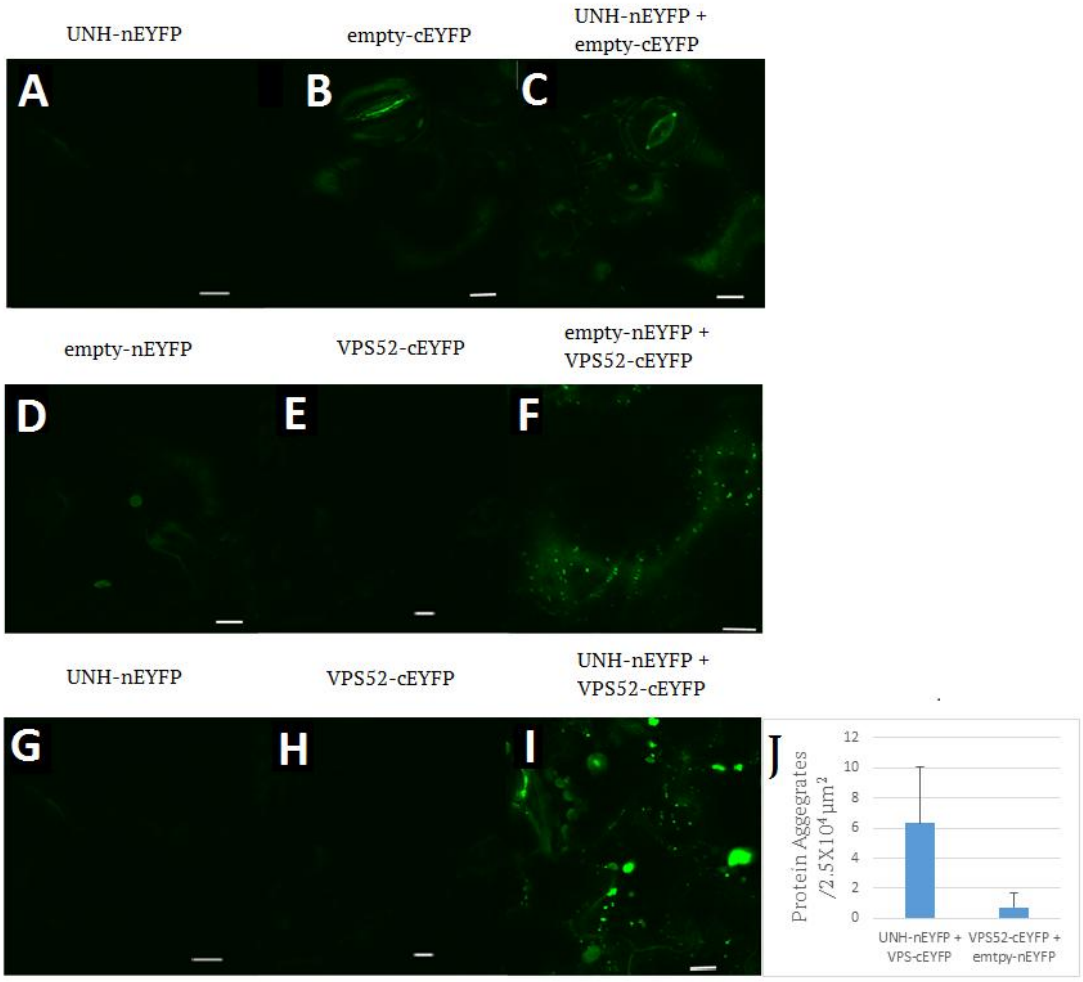

Figure 21. Confocal images of the sub-cellular localization of transiently expressed UNHINGED with VPS52. Tobacco expressing plasmids listed as follows. First row: (A) UNH-nEYFP, (B) empty-cEYFP and (C) UNH-nEYFP + empty-cEYFP. Second row: (D) empty-nEYFP, (E) VPS52-cEYFP and (F) empty-nEYFP + VPS52-cEYFP. Third row: (G) UNH-nEYFP, (H) VPS52-cEYFP and (I) UNH-nEYFP + VPS52-cEYFP. (J) Graph indicating number of protein aggregates in epidermal tobacco cell areas (n=15) of VPS52-cEYFP and empty-nEYFP (I) vs UNH-nEYFP (F). All plasmids listed were expressed in tobacco epidermal cells. Scale bar: 10 µM.

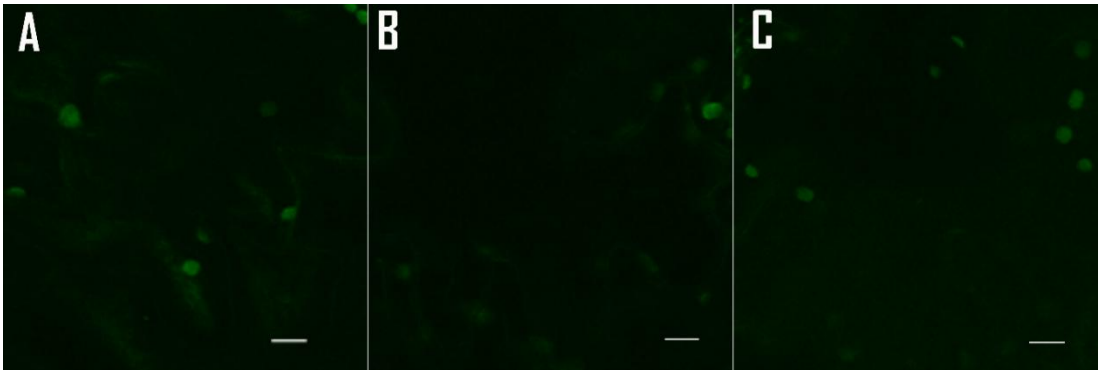

Figure 22. Confocal images of the sub-cellular localization of transiently expressed UNHINGED-nEYFP(A) with SYP61-cEYFP (B) in tobacco epidermal cells. C reveals A and B being co-expressed. Scale bar: 10 µM.

Appendix 1

Infiltration Buffer – 1 mL Na_3PO_4 20 mM, 1 mL MES 500 mM, 10 µL Acetosyringone in DMSO 200 mM, 50 mg D-Glucose, add water to 10 mL.

LB media (1 L) – 800 mL distilled water with 10 g Bacto-tryptone, 5 g Yeast extract, 5 g NaCl, filled to 1 L water (add 15 g agar for plates).

LiAc solution pH 7.5 (5 mL) – 0.5 mL 10x (1 M) LiAc, 0.5 mL 10x TE (0.1 M Tris-HCl, 0.01 M EDTA pH 8 with HCl), 4 mL sterile water

Transformation Mix (1 rxn) – 240 µL 50% PEG, 36 µL 1.0M LiAC, 50 µL boiled SS-carrier DNA, 34 µL plasmid DNA and water.

SD media (1 L) – 20 g D-glucose anhydrous, 6.7 g nitrogen base, 1.5 g drop-out powder

S.O.B. (100 mL) – 90 mL distilled water, 2 g bacto-tryptone, 0.5 g yeast extract, 0.2 mL NaCl (5 M), 0.25 mL KCl (1 M), 0.10 mL $MgCl_2$ (1 M), 0.10 $MgSO_4$ (1 M), 2 mL D-glucose (1 M), fill to 100 mL, filter sterilize. For transformation use S.O.C. by adding 9.5 µL 2M glucose to 950 mL S.O.B.

TE Buffer – 10 mM Tris-HCL (pH 8.0), 1 mM Na-EDTA (pH 8.0)

Z-buffer – 60 mM Na_2HPO_4, 40 mM NaH_2PO_4, 10 mM KCl, 1 mM $MgSO_4$, to be stored at 4^{o}C until use, then add 2.7 µL β-mercaptoethanol/mL, and 1 mg/mL X-gal